OLD DOMINION UNIVERSITY RESEARCH FOUNDATION

DEPARTMENT OF MATHEMATICAL AND COMPUTING SCIENCES
SCHOOL OF SCIENCES AND HEALTH PROFESSIONS
OLD DOMINION UNIVERSITY
NORFOLK, VIRGINIA

LONG-TERM RADIATION EFFECTS ON GaAs SOLAR CELL CHARACTERISTICS

By

John H. Heinbockel

and

M. J. Doviak

Final Report
For the period June 1, 1977 - May 31, 1978

Prepared for the
National Aeronautics and Space Administration
Langley Research Center
Hampton, Virginia 23665

Under
Research Grant NSG 1426
Edmund J. Conway, Technical Monitor
Space Systems Division

May 1978

DEPARTMENT OF MATHEMATICAL AND COMPUTINC SCIENCES
SCHOOL OF SCIENCES AND HEALTH PROFESSIONS
OLD DOMINION UNIVERSITY
NORFOLK, VIRGINIA

LONG-TERM RADIATION EFFECTS ON GaAs SOLAR CELL CHARACTERISTICS

By

John H. Heinbockel

and

M. J. Doviak

Final Report
For the period June 1, 1977 - May 31, 1978

Prepared for the
National Aeronautics and Space Administration
Langley Research Center
Hampton, Virginia 23665

Under
Research Grant NSG 1426
Edmund J. Conway, Technical Monitor
Space Systems Division

Submitted by the
Old Dominion University Research Foundation
Norfolk, Virginia 23508

May 1978

ACKNOWLEDGMENTS

The authors would like to thank E. Conway, G. Walker, and C. Byvick of NASA/Langley Research Center for their comments and discussions during the course of this study. We would also like to thank E. Gillard, J. Nodurft, and A. Tennille of Old Dominion University Research Foundation.

TABLE OF CONTENTS

LIST OF TABLES

LIST OF FIGURES

(continued)

LIST OF FIGURES (concluded)

LONG-TERM RADIATION EFFECTS ON GaAs SOLAR CELL CHARACTERISTICS

By

J.H. Heinbockel[1] and M.J. Doviak[2]

SUMMARY

This report investigates preliminary design considerations which should be considered for a space experiment involving Gallium Arsenide (GaAs) solar cells. The electron radiation effects on GaAs solar cells were conducted in a laboratory environment, and a statistical analysis of the data is presented. In order to augment the limited laboratory data, a theoretical investigation of the effect of radiation on GaAs solar cells is also developed. The results of this study are empirical prediction equations which can be used to estimate the actual damage of electrical characteristics in a space environment. The experimental and theoretical studies also indicate how GaAs solar cell parameters should be designed in order to withstand the effects of electron radiation damage.

[1] Professor of Mathematics and Computing Sciences, School of Sciences and Health Professions, Old Dominion University, Norfolk, Va. 23508

[2] Assistant Professor of Mathematics and Computing Sciences, School of Sciences and Health Professions, Old Dominion University, Norfolk,

INTRODUCTION AND STATEMENT OF THE PROBLEM

This study was initiated to investigate preliminary design considerations for a space experiment on GaAs solar cells. The first steps in the design of a space experiment on GaAs solar cells are to identify the experiment goals and determine the need for a space experiment. The actual feasibility of a space experiment and the conceptual design of a flight package are not considered in this study.

In developing the goals of a space experiment consideration should be given to the advantages which GaAs solar cells offer over other types of solar cells. These advantages are (1) higher AM-0 efficiency, (2) greater stability in a space radiation environment and (3) operating capability up to 300° C.

The need for a space experiment arose from two needs. First, laboratory measurements can be made which accurately compare different solar cell types. However, reliable data is needed to show how GaAs solar cells perform in a real space orbit rather than in an environment imperfectly simulated in a laboratory. Secondly, a functioning demonstration is needed to convince spacecraft designers that GaAs solar cells are ready for use in space power systems.

The first experimental goal became the measurement of the power-generating capability of GaAs solar cells when exposed to a space radiation environment. Data on the effects of radiation on GaAs solar cells was just becoming available when this study was initiated. The data was generated through NASA/Langley Research Center and contractual efforts. Some limited data was also available through independent programs.

The second experimental goal was the measurement of power generation in GaAs solar cells at elevated temperature and various sun intensities in space. A review of the available data on elevated temperature operations of GaAs solar cells indicated that insufficient data existed to plan a 300°C space experiment. The need for such an experiment was demonstrated through intensive laboratory research. Because data is just now becoming available, the high temperature study is not considered in this report.

LIST OF SYMBOLS

q	electron charge = $1.602192(10^{-19})$ [Coulomb]
F_o	density of incident photons per unit time per unit bandwidth
R	fraction of photons reflected from surface
C	speed of light = $2.997(10^{8})$ [ms^{-1}]
ϕ	fluence [electrons/cm^2]
N_a	number of acceptors on p-side
N_d	number of donors on n-side
n_i	intrinsic carrier density
K	Boltzman's constant = $1.38(10^{-23})$ [JK^{-1}]
h	Planck's constant = $6.6262(10^{-34})$ [Js]
M_n^*, M_p^*	effective masses of holes and electrons [kg]
M_o	electron rest mass = $9.109558(10^{-31})$ [kg]
E_g	band gap energy [eV]
T	temperature [°K]
ε_o	permitivity of GaAs [F/cm]
D	window thickness [cm]
μ_n, μ_p	mobilities of minority carriers [cm^2/volt-sec]
x_1, x_j	junction depth [μm]
W	width of depletion region [cm]
H	total cell thickness [cm]
S_a, S_g, S_p	recombination velocities [cm/sec]
τ_a, τ_g, τ_p	lifetimes of minority carriers [sec^{-1}]
D_a, D_g, D_p	diffusion coefficients [cm^2/sec]

L_a, L_g, L_p	diffusion lengths [cm]
α, β	absorption coefficients for GaAs and GaAlAs [cm^{-1}]
J	photocurrent density [mAmps/cm^2]
I_{sc}	short-circuit current density [mAmps/cm^2]
SR	spectral response
$P(\lambda)$	average spectral irradiance at 1.A.U. [W cm^{-2} μm^{-1}]
E	photon energy [eV]
λ	wavelength [μm]
V_{oc}	open circuit voltage [V]
V_o	theoretical maximum open circuit voltage [V]
Y_i	response of dependent variable
β_i	unknown parameters
ϵ_i	normally distributed random variable
$\underline{Y}$, $\underline{\beta}$, $\underline{\epsilon}$	column vectors
σ	standard deviation

STATISTICAL ANALYSIS OF GaAs SOLAR CELL DATA

Introduction

The next several sections will discuss the effects of 1 MeV electron irradiation on the performing capabilities of GaAs solar cells. In the following analysis the cell junction depth x_i (2 levels) and fluence ϕ (4 levels) will be the independent variables. The ratios (I_{sc}/I_{sco}, V_{oc}/V_{oco}) of short-circuit current and open-circuit voltage after irradiation to that before irradiation will be the measures of the solar cell degradation and will be the dependent or response variables. The analysis consists of performing a multiple regression analysis to relate

I_{sc}/I_{sco} and V_{oc}/V_{oco} to both x_1 and ϕ. The resulting prediction equations then can be invoked together with estimates of electron flux in appropriate orbits to predict decreases in the short circuit-current and open-circuit voltages for various orbital periods. Residual analyses and tests for lack of fit are performed to check the adequacy of the models as well as underlying assumptions.

Due to the complex functional relationships existing between the aforementioned variables, the models developed are empirical in nature. Many models were entertained before formulating the final models presented in this report. Many models were rejected due to a poor fit or intractable analysis. When used properly, the final models presented in this report will provide good predictions for the response variables. These models fit the experimental data well and are also relatively concise.

Description of Experiment

The experimental units in the experiment consisted of 45 heterofaced p-GaAlAs/p-GaAs/n-GaAs solar cells fabricated using the etch back epitaxy process. A detailed account of the growing process may be found in reference 1. Large area vacuum evaporated Sn-Ag contacts were used for electrical connection to the N-GaAs. The front finger contacts were spurted Pd-Ag.

The solar cells were mounted on aluminum backing plates and then irradiated with 1 MeV electrons. Groups of cells were irradiated at fluences of 10^{13}, 10^{14}, 10^{15} and 10^{16} electrons/cm^2. The short-circuit currents as well as the open-circuit voltages were measured before and after irradiation.

Due to lose connections during the measuring process, some faulty data was obtained. Thirty-four measurements on short-circuit current and 32 measurements on open-circuit voltage remained after the faulty data was discarded. Each cell had a junction depth of either 1.5 or 4.0 microns and was subjected to one of the 4 fluences of 1 MeV electrons as mentioned above.

Experimental error explains different values of the dependent variable occurring at the same setting of the independent variables and occurs because of factors beyond the control of the experimenter. Some of these factors are the technique of growing the cells, heterogeneity of the experimental units, differences in the amount of irradiation administered, mechanical failures and measurement errors.

Results of Regression Analysis

Let Y_i, $i = 1,2,\ldots, n$ denote a response or dependent variable that is measurable. We assume that a relationship of the following form exists between the independent variables and dependent variables:

$$Y_i = \beta_0 + \beta_1 x_{i1} + \ldots + \beta_k x_{ik} + \varepsilon_i, \quad i = 1,2,\ldots, n$$

where $\beta_0, \beta_1,\ldots, \beta_k$ are unknown parameters, $x_{i1},\ldots,x_{ik}$ are known values of the k independent variables and ε_i is a normally distributed random variable with mean 0 and unknown variance σ^2 [written $\varepsilon_i \sim N(0,\sigma^2)$].

The above model is a linear model, since it is linear in the parameters, and it can be represented in the matrix notation

$$\underset{\sim}{Y} = X \underset{\sim}{\beta} + \underset{\sim}{\varepsilon} \tag{1}$$

where $\underset{\sim}{Y}' = [Y_1, Y_2,\ldots, Y_n]$, $\underset{\sim}{\beta}' = [\beta_0, \beta_1,\ldots, \beta_k]$, $\underset{\sim}{\varepsilon} = [\varepsilon_1, \varepsilon_2, \ldots, \varepsilon_n]$ and X is an $n \times (k + 1)$ matrix with typical element x_{ij} ($x_{io} = 1$ for all i). The ε_i's are independent and identically distributed normal variables with mean 0 and variance σ^2. The variance-covariance matrix of $\underset{\sim}{\varepsilon}$ given by $\sigma^2 I$ where I is the $n \times n$ identity matrix.

Assuming that $X'X$ is nonsingular, the least squares estimator for $\underset{\sim}{\beta}$ is given by (refs. 2,3):

$$\underset{\sim}{b} = (X'X)^{-1} X' \underset{\sim}{Y} \tag{2}$$

$$\hat{\sigma}^2 = [\underset{\sim}{Y}'\underset{\sim}{Y} - \underset{\sim}{b}'X'\underset{\sim}{Y}] \div [n - (k + 1)]. \tag{3}$$

Although they will not be presented here, the estimators $\underset{\sim}{b}$ and $\hat{\sigma}^2$ possess many desirable properties from a statistical standpoint. The equation

$$\hat{Y} = \underset{\sim}{b}'\underset{\sim}{X}_o \tag{4}$$

is called a prediction equation and may be used to predict future responses of the dependent variable at $\underset{\sim}{X}_o$, the desired setting of the independent variables. A $(1 - \alpha)$ 100 percent prediction interval for a future response Y at $\underset{\sim}{X}_o$ is given by

$$\hat{Y} \pm t_{\alpha/2,\ \nu}\ \hat{\sigma}[1 + \underset{\sim}{X}_o'(X'X)^{-1}\ \underset{\sim}{X}_o]^{1/2} \tag{5}$$

where $t_{\alpha/2,\ \nu}$ is obtained from a table containing probabilities for students' -t distribution.

In some instances the variance-covariance matrix of $\underset{\sim}{\varepsilon}$ is not $\sigma^2 I$ but instead $\sigma^2 V$ where V may have nonzero off diagonal elements (implying correlations between responses) or unequal diagonal elements (implying some responses are more variable than others). In these instances a weighted least square analysis is needed to determine equations (2), (3) and (5), and these formulas must be accordingly modified to read

$$\underset{\sim}{b} = (X'V^{-1}X)^{-1}X'V^{-1}\underset{\sim}{Y} \tag{6}$$

$$\hat{\sigma}^2 = \underset{\sim}{Y}'V^{-1}\ \underset{\sim}{Y} - \underset{\sim}{b}'X'V^{-1}\ \underset{\sim}{Y} \tag{7}$$

and

$$\hat{Y} \pm t_{\alpha/2,\ \nu}\ \hat{\sigma}[V_i + \underset{\sim}{X}_o'(X'V^{-1}\ X)^{-1}\ \underset{\sim}{X}_o]^{1/2} \tag{8}$$

respectively, where $V_i\sigma^2$ is the variance of $\underset{\sim}{Y}$ at $\underset{\sim}{X}_o$.

For the short-circuit current data the following model is assumed:

$$Y_i = \beta_0 + \beta_1 x_{i1} + \beta_2 x_{i2} + \varepsilon_i \quad i = 1, \ldots, 34 \tag{9a}$$

where $Y_i = \log_{10}\left(\frac{I_{sco}}{I_{sc}} - 1\right)$, x_{i1} = junction depth of cell i and $x_{i2} = \log_{10}[\phi/10^{16}]$ with ϕ the fluence. The matrix V^{-1} is assumed to be a diagonal matrix with diagonal elements

$$d_{11} = d_{22} = 0.0876$$
$$d_{33} = d_{44} = d_{13,13} = 1.413$$
$$d_{14,14} = \ldots = d_{19,19} = 0.3532$$
$$d_{20,20} = \ldots = d_{23,23} = 0.1554$$

and $d_{24,24} = \ldots = d_{34,34} = 1.413$

The weighted least squares estimate of $\underset{\sim}{\beta}$ is computed to be

$$\underset{\sim}{b} = \begin{bmatrix} 0.8649 \\ 0.1940 \\ 1.075 \end{bmatrix} \quad \text{and} \quad \hat{\sigma} = 0.138$$

which gives a prediction equation of

$$\hat{Y} = 0.8649 + 0.194x_1 + 1.075x_2 \tag{9b}$$

or

$$\frac{I_{sc}}{I_{sco}} = \frac{1}{1 + \left(10^{0.8649 + 0.194x_1}\right)\left(\frac{\phi}{10^{16}}\right)^{1.075}} \tag{9c}$$

A plot of equations 9a to 9c is given in figure 1.

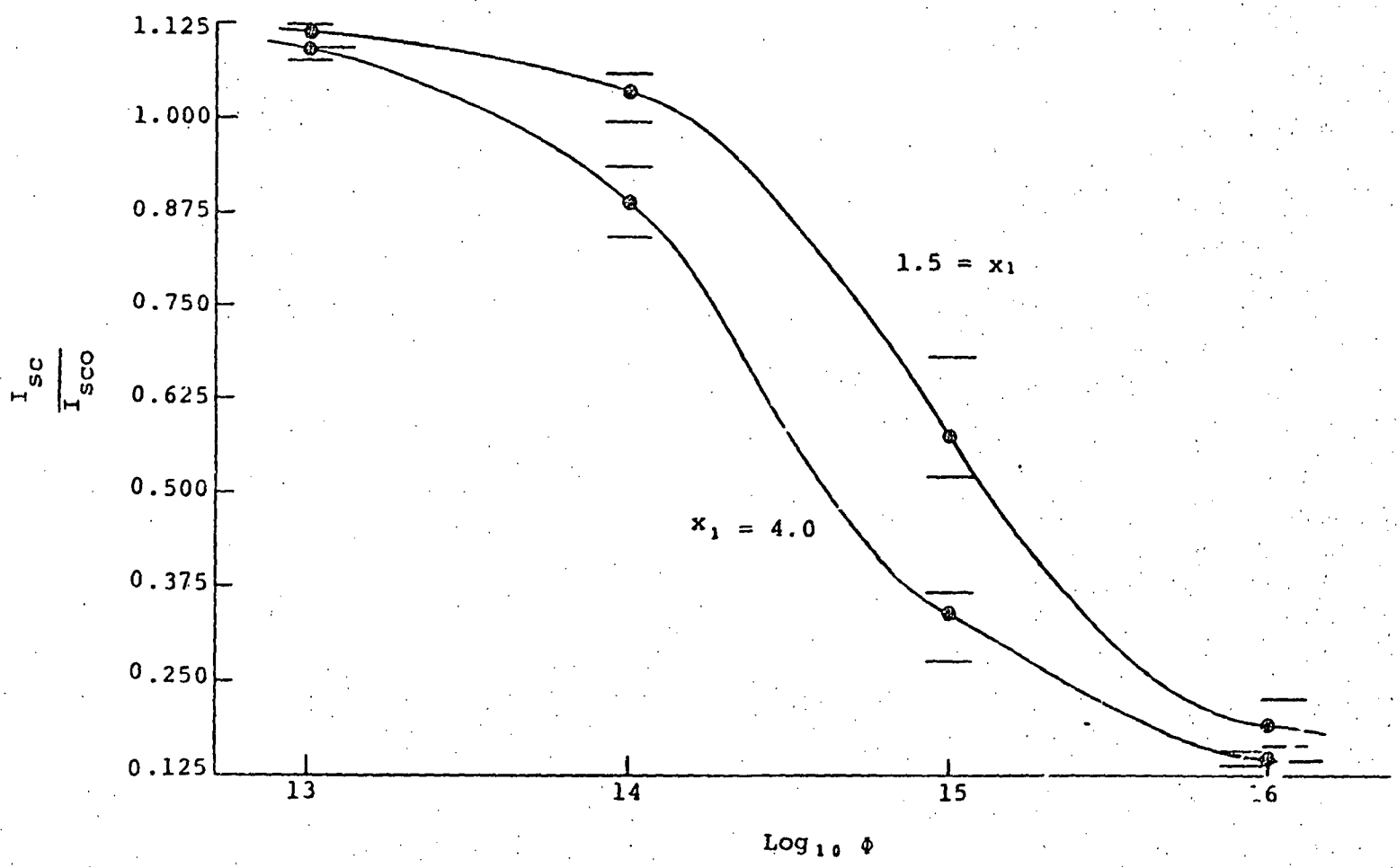

Figure 1. Prediction equation for I_{sc}/I_{sco} vs. fluence for 1 MeV electron irradiation at various junction depths.

Prediction Interval

Let $x_1 = 0.8$ μm and $x_2 = -2$ ($\phi = 10^{14}$). Then a point predictor for a future response Y is given by -1.1299 and thus a point predictor for I_{sc}/I_{sco} is calculated to be 0.931. A 95 percent prediction interval for Y is given by

$$-1.1299 \pm 2.041(0.138)[1.413 + \underset{\sim}{X}_o'(\underset{\sim}{X}'V^{-1}\underset{\sim}{X})^{-1}\underset{\sim}{X}_o]^{1/2}$$

where 2.041 is the tabulated t-value, 1.413 is an estimate of V_i and 0.138 is the computed estimate of σ. The above reduces to

$$-1.1299 \pm 2.041(0.136)[1.413 + 0.112]^{1/2}$$

or

$$(-1.478, -0.782)$$

which is the prediction interval for Y. This gives a 95 percent prediction interval for I_{sc}/I_{sco} of (0.858, 0.967).

The quantity $Y_i - \hat{Y}$, $i = 1,2,\ldots,34$ is called the ith residual and gives the difference between the ith value of the response variable and the value of the prediction equation. Plotting the residuals against various quantities provides a graphical method of checking whether the prediction equation fits the data well and also whether the underlying assumptions for the analysis are violated. Figure 2 gives the weighted residuals for the short-circuit current data. These residuals are plotted against $\hat{Y}$, and, with the exception of one point, the residuals tend to fall in a horizontal band around the Y-axis. If an unweighted analysis were performed, the variance of the residuals would differ significantly and they would not have the horizontal band appearance which is desirable. Also, because there is no curvature present in the residuals, the prediction equation fits the data well.

The analysis of variance for the regression analysis is given in table 1.

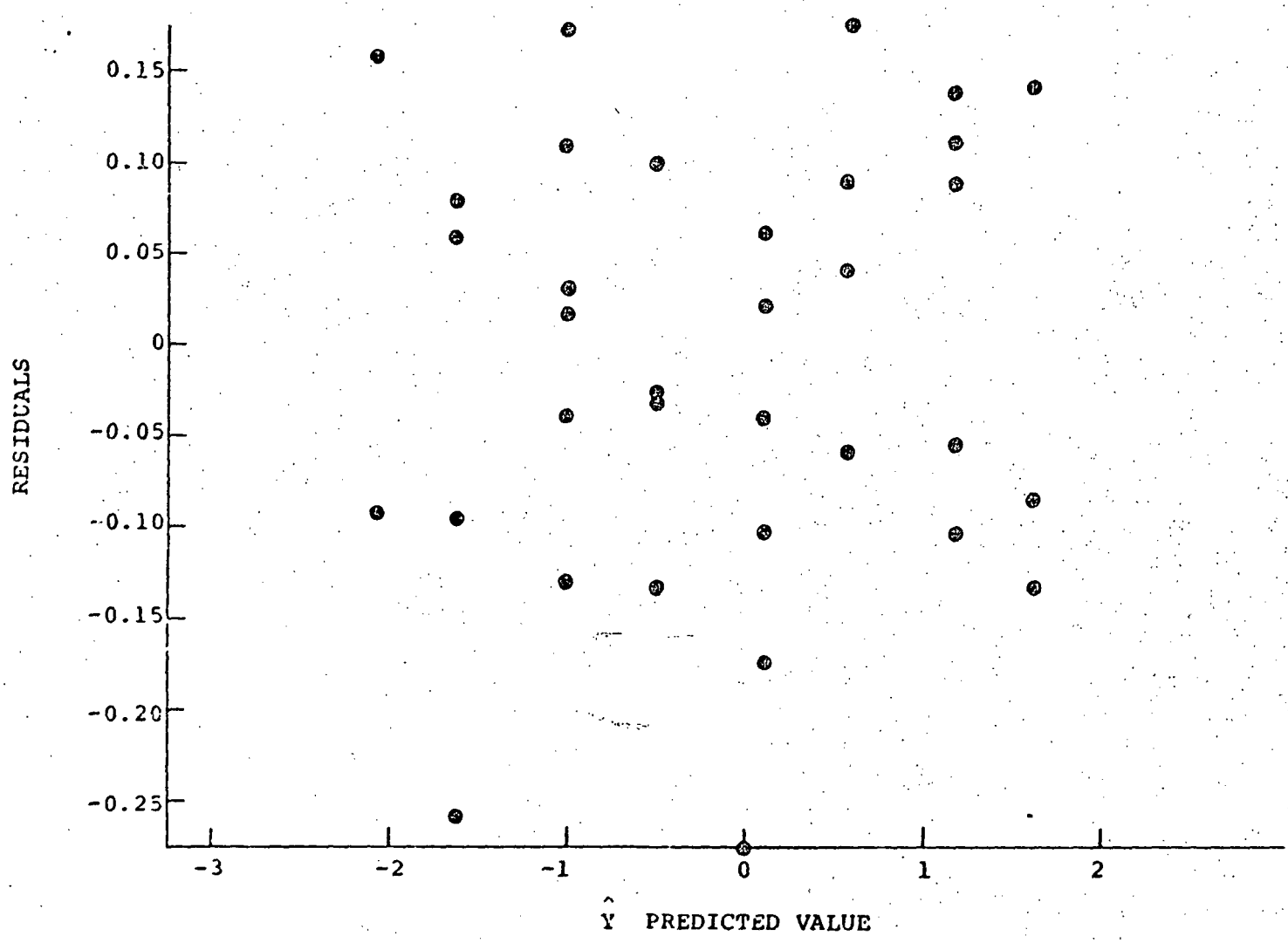

Figure 2. Plot of residuals vs. predicted values (short-circuit current).

Table 1. Analysis of variance for regression analysis of I_{sc}/I_{sco}; DF = degrees of freedom, SS = sum of squares of error, MS = mean square error, and F = F-statistic.

Source	DF	SS	MS	F
Regression	2	28.255	14.128	761.317
Residuals	31	0.575	0.019	
Total	33	28.830		

In table 1 the F-statistic of 761.317 is highly significant, meaning that the junction depth and fluence terms should be included in the model. A more extensive analysis of variance, which decomposes the residual sum of squares into sum of squares pure error and sum of squares lack of fit, is given in table 2.

Table 2. More extensive analysis of variance; DF = degrees of freedom, SS = sum of squares of error, MS = mean square error, and F = F-statistic.

Source	DF	SS	MS	F
Regression	2	28.255	14.128	761.317
Residual	31	0.575	0.019	
Lack of fit	5	0.071	0.014	0.74
Pure error	26	0.504	0.019	

The additional F-value in table 2 is a test statistic for testing for a lack of fit in the model. Had this value exceeded the tabulated value of $F_{0.05,5,26} = 2.59$ then lack of fit could be concluded. However, since $0.74 < 2.59$ there is no evidence of lack of fit.

Open-Circuit Voltage Model

A similar regression analysis was performed on the open-circuit voltage data. Several models were considered before a satisfactory

fit to the data was found. The model of equation (9) with $Y_i = \log_{10}\left(\frac{V_{oco}}{V_{oc}} - 1\right)$ was fitted to the data; however, a plot of residuals versus fluence suggested that a quadratic term in the fluence be added to the model. The resulting model is

$$Y_i = \beta_0 + \beta_1 x_{i1} + \beta_2 x_{i2} + \beta_3 x_{i2}^2 + \varepsilon_i, \quad i = 1, \ldots, 32 \qquad (10a)$$

where $Y_i = \log_{10}\left(\frac{V_{oco}}{V_{oc}} - 1\right)$, x_{i1} = junction depth of cell i and $x_{i2} = \log_{10}[\phi/10^{16}]$. Again it was necessary to use least squares with weights given by

$$d_{11} = \ldots = d_{66} = 0.062, \; d_{77} = \ldots = d_{11,11} = 0.25$$

$$d_{12,12} = \ldots d_{17,17} = 1, \; d_{18,18} = \ldots = d_{21,21} = 25$$

$$d_{22,22} = \ldots = d_{25,25} = 0.64, \; d_{26,26} = \ldots = d_{29,29} = 1$$

and $d_{30,30} = \ldots = d_{32,32} = 0.64$. The least squares estimate of $\underset{\sim}{\beta}$ was computed to be

$$\underset{\sim}{b} = \begin{bmatrix} -0.6037 \\ 0.098 \\ 0.609 \\ 0.060 \end{bmatrix}$$

which gives a prediction equation of

$$\hat{Y} = -0.6037 + 0.098x_1 + 0.609x_2 + 0.060x_2^2 \qquad (10b)$$

The predicted values of V_{oc}/V_{oco} at the different junction depth-fluence combinations is illustrated in figure 3. An examination of the residuals in figure 4 shows no glaring abnormalities.

The analysis of variance for the regression analysis is presented in table 3.

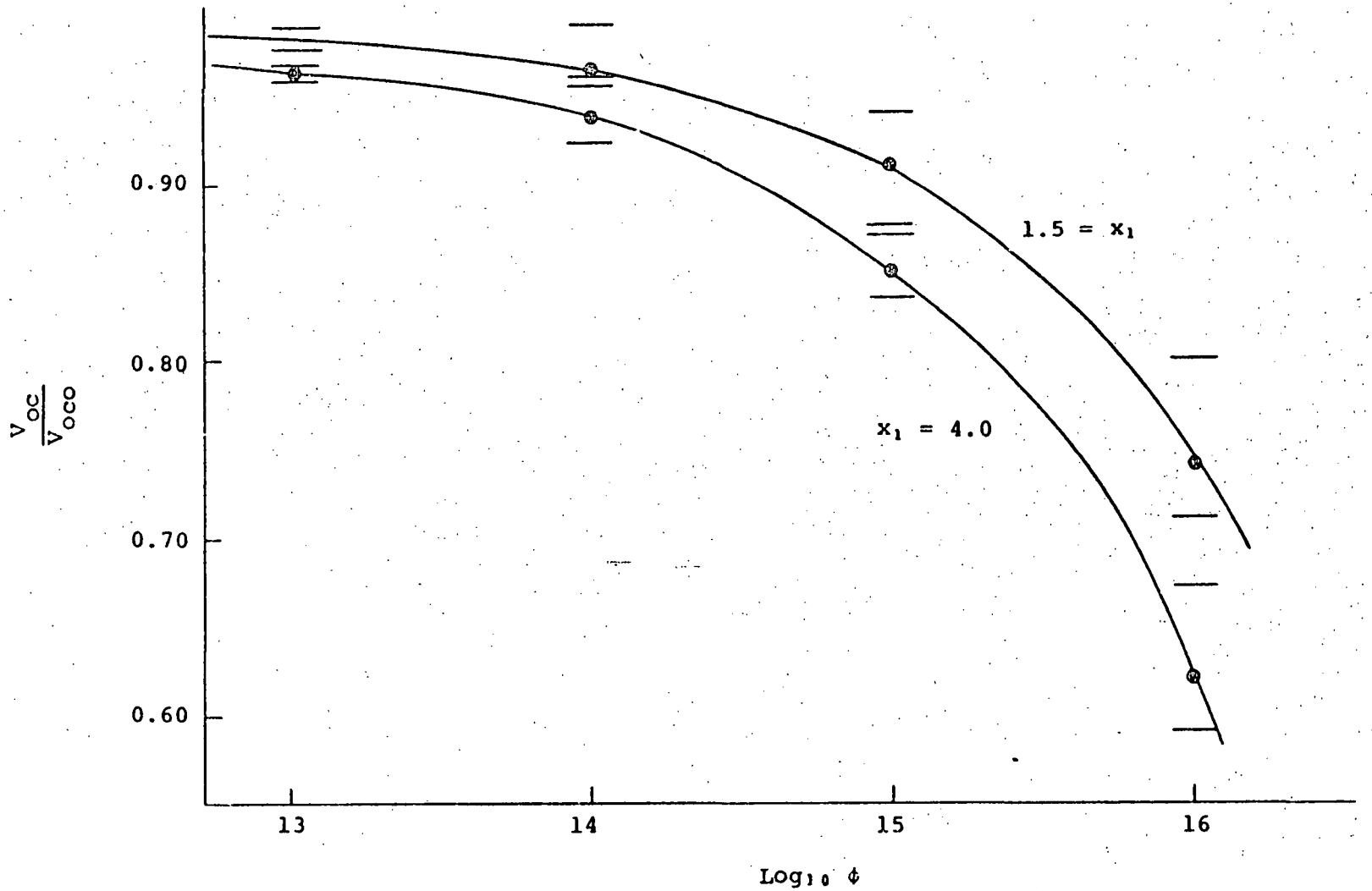

Figure 3. Prediction equation for V_{OC}/V_{OCO} vs. fluence for 1 MeV electron irradiation at various junction depths.

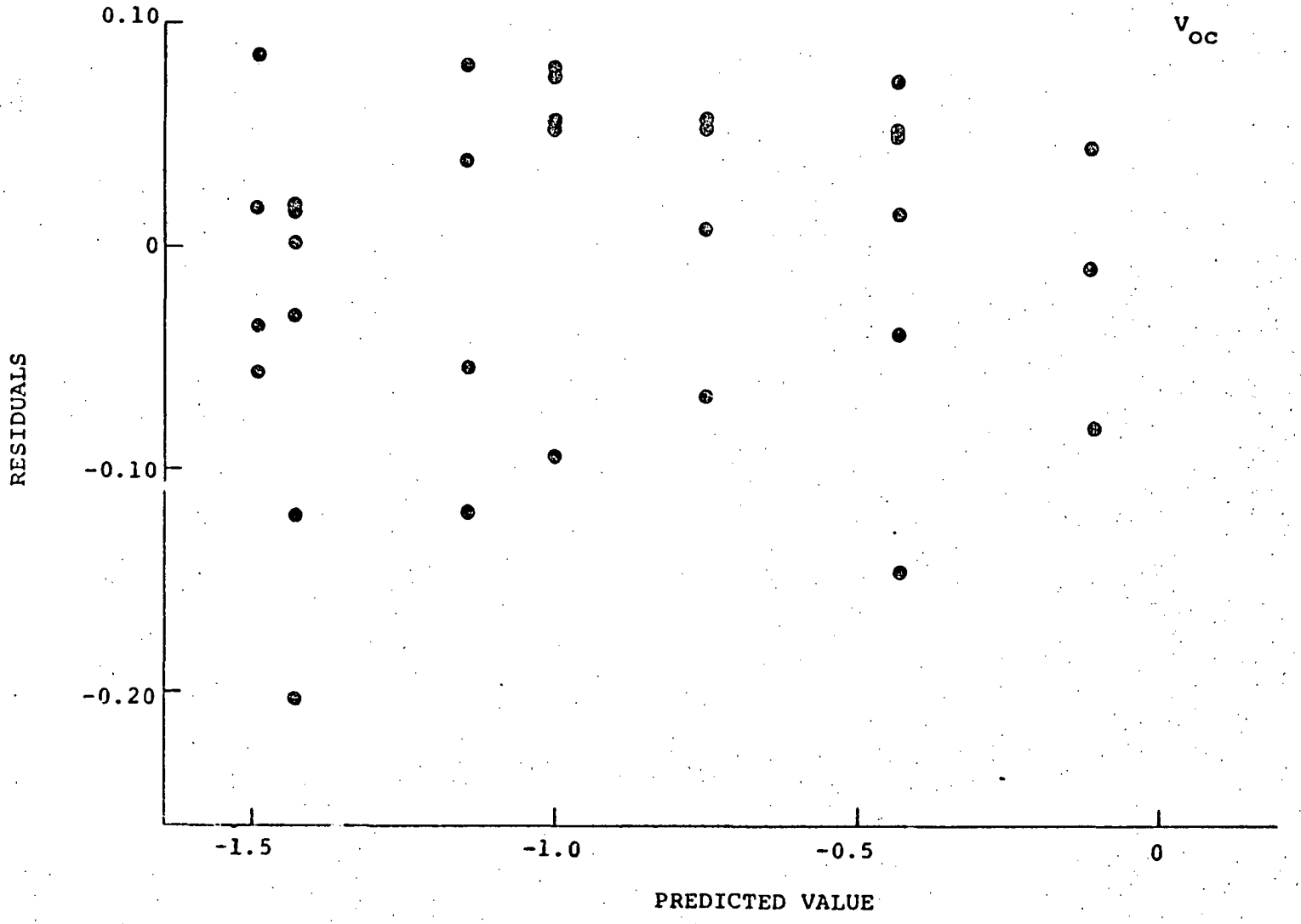

Figure 4. Plot of residuals vs. predicted values (open-circuit voltage).

Table 3. Analysis of variance for regression analysis of V_{oc}/V_{oco}; DF = degrees of freedom, SS = sum of squares of error, MS = mean square error, and F = F-statistic.

Source	DF	SS	MS	F
Regression	3	2.988	0.996	571.219
Residuals	28	0.049	0.002	
Lack of fit	3	0.007	0.0023	1.43
Pure error	25	0.042	0.0016	
Total	31	3.037		

In table 3 the F-statistic of 571.219 is good and the F-statistic testing for lack of fit is not significant at $\alpha = 0.05$, which indicates there is no lack of fit. When the model was fitted without the quadratic term there was, at $\alpha = 0.05$, evidence of lack of fit.

SPACE EXPERIMENT CONSIDERATIONS

The following is an outline of statistical considerations that must be incorporated into an in-space experiment for comparing GaAs solar cells with other varieties of solar cells. In particular, we will discuss in a rather general way such things as: the design model and assumptions associated with an experiment; a discussion of the data analysis; and sample size considerations. Finally we will summarize the proposed techniques.

Let I_{sc}/I_{scc}, which denotes the ratio of the short-circuit current after irradiation to that before irradiation, be a measure of the solar cell degradation. (We could also use maximum power ratio or open-circuit voltage ratio as a measure of solar cell degradation.) Let I_{sc} denote the short-circuit current measured at some point during or at the conclusion of a space flight. We let p denote the number of types of cells included in the experiment. The cells

will be either GaAs or S_i, and some may be chosen to be annealed. In any case there will be p different types of solar cells under consideration.

Notationally we let μ_i, $i = 1,2,\ldots, p$ be the average value of I_{sc}/I_{sco} for cell type i at the designated orbit where the average is based on a hypothetical population of cells. Actual responses of I_{sc}/I_{sco} may differ considerably from the corresponding μ_i due to experimental error which is composed of: measurement error, cell heterogeneity, faulty connections, and different amounts or types of irradiation. Even though experimental errors exist we can still make inferences about the μ_i's and more specifically about $\mu_i - \mu_j$, $i \neq j$.

Previous sections are of a rather general nature, partially because little is known concerning the proposed flight at this time. More specific recommendations could be made as the decisions on the proposed flight become finalized. The following decisions need to be made concerning an experimental design:

(a) What area is available for solar cells onboard the space vehicle and the number of cells that can be mounted on this area, and

(b) whether the experiment is to be a multi-factor experiment (with three factors: (1) junction depth (2) type of cell, S_i or GaAs, and (3) whether cells are annealed or not annealed).

If a multi-factor experiment is desired the considerations discussed earlier should be changed accordingly. However, the previous discussion on sample size will still be applicable. In any case, the goals of a proposed experiment must be specifically stated prior to the experimental design stage.

Experimental Design

The only apparent source of variation , other than those listed above, contributing to experimental error is due to solar cell (treatment) differences. Therefore a completely randomized design is a logical choice. This means that if n cells (assuming that the same number of cells of each type will be included) should

be randomly chosen from all available cells of each type, there will result np experimental units in the experiment. A table of random numbers (or similar device) should be consulted to guarantee random samples.

The probabilistic model associated with a completely randomized design is given by

$$Y_{ij} = \mu_i + \varepsilon_{ij} \quad i = 1,2,\ldots,p \quad j = 1,2,\ldots, n$$

where Y_{ij} is the jth response (value of I_{sc}/I_{sco} or some other measure) at treatment i, the μ_i's are the unknown treatment means, and ε_{ij} is the random error associated with the measurement Y_{ij}. It is assumed that for all i and j, ε_{ij} is a normal random variable with mean and variance o and σ^2, respectively. It is also assumed that any pair of ε's are uncorrelated random variables.

If it is suspected that the variance of the response changes with treatments, then an appropriate transformation of the data should be made in order to stabilize the variance. This technique was used in the regression analysis of the terrestial data. If the data is transformed it is noted that the resulting confidence intervals apply to the transformed and not to the original parameters.

ANALYSIS OF DATA

The first step in the statistical analysis is to perform a one-way analysis of variance on the data. This entails decomposing the total sum of squares of error $\left(\text{total SS} = \sum\sum_{ij} (Y_{ij} - \bar{Y})^2\right)$ into treatment sums of squares $\left(\text{SST} = \sum_i n(\bar{Y}_i - \bar{Y})^2\right)$ and error sum of squares (SSE = total SS minus treatment sum of squares), where $\bar{Y} = \sum\sum_{ij} Y_{ij}/n\ p$ and $\bar{Y}_i$ is the mean of the observations for cell-type i. The results are summarized in the following analysis of variance (ANOVA) table:

ANOVA

Source	DF	SS	MS	F
Treatments	p-1	SST	MST	MST/MSE
Error	np-p	SSE	MSE	
Total	np-1	Total SS		

The abbreviation DF appearing in the table denotes "degrees of freedom," the parameter of a x^2 random variable. The MS column is obtained by dividing SS by the appropriate DF. If F = MST/MSE is "small" (smaller than a tabulated F value, based on p-1 and ν = np-p degrees of freedom) then it is concluded that no difference exists in the treatment means and the analysis is complete. If the F-statistic is larger than the tabulated value it is concluded that not all the μ_i's are equal.

When the F-statistic is significant (large) it is usually desirable to determine just where the differences lie in the μ_i's. The statistical techniques appropriate for this type of analysis are collectively known as multiple comparison procedures (see ref. 4). Some of the multiple comparison methods in common use include: the Least Significant Difference, Scheffe's Method, Tukey's Method, the Student-Newman-Keuls Method, Duncan's Method, and Dunnett's Method. The appropriate method in any situation depends upon the overall goals of the experiment and should be chosen accordingly. Although it is not obvious (see ref. 5) which procedure is appropriate in some experiments, the Tukey procedure is a likely choice for the experiment under consideration. It ranks high in controlling the experimentwise error rate (ref. 5) and is particularly good if we wish to find confidence intervals for the differences in treatment means. Briefly, the procedure may be outlined as follows: set an appropriate confidence coefficient 1 - α. (This is the probability that all the confidence intervals constructed will contain the respective parameters.) Obtain the quantity $Q(1 - \alpha, p, \nu)$ from special studentized range tables (ref. 5). Compute $Q(1 - \alpha, p, \nu)\ (MSE/n)^{1/2} = D$. Construct a confidence interval of any difference $\mu_i - \mu_j$ by calculating

$$\bar{Y}_i - \bar{Y}_j \pm D.$$

Do this for any differences of interest. If a particular interval does not contain the point "zero," the means are concluded to be different.

Sample Size Considerations

Choosing the optimum number of cells of each type to include in the experiment is an important consideration in the design of the experiment. If cost, weight, and available space restrictions did not exist, the more cells included in the experiment the better the inferences that could be made. Since this is not the case, the sample sizes should be chosen to satisfy some criterion (or criteria) specified by the experimenter. One such criterion is to choose the n_i's so that the confidence interval widths (or half-widths) for the differences in the means is less than some bound (specified by the experimenter) with probability $1 - \alpha$. The choice of the appropriate bound is important. If chosen to be too large, the confidence intervals will be too wide and imprecise inferences will result. Too small a bound will yield inordinately large sample sizes. Some compromise is needed. For example, it may be desirable that the half-width of any confidence interval for $\mu_i - \mu_j$ not exceed 0.03 and that this will occur with probability $1 - \alpha = 0.90$. The optimum value for n can be obtained by solving

$$0.03 = Q(0.90, p, \nu)\ (MSE/n)^{1/2}$$

for n. For illustrative purposes assume that $p = 8$ and $\phi \approx 10^{14}$ (or some equivalent value when considering other types of irradiation). Also assume a junction depth of 1.5. Then approximating $MSE^{1/2}$ by 0.022 (based on the terrestial data) gives

$$0.03 = Q(0.90, 8, 8(n - 1))\frac{0.022}{\sqrt{n}}$$

Consulting a studentized range table and solving for n gives the optimal n as approximately 8. Therefore if 8 cells of each type are included in the experiment the probability is 0.90 that all half-widths of the confidence intervals will not exceed 0.03.

Actually, during the space flight a cell may incur any of a number (say k) of types of malfunctions which may render the cell inoperable or make it impossible to obtain a measurement on the cell. In this case it would be reasonable to include n' cells of each type in the experiment where n' is some number larger than the optimal number derived in the previous paragraphs. A method for approximating n' is now given.

Notationally, let p_i $i = 1, 2, \ldots, k$ denote the probability that any cell incurs malfunction i during flight. Assuming that the types of malfunctions are independent events, the probability that a cell incurs no malfunctions during flight is given by

$$q = \prod_{i=1}^{k} (1 - p_i) .$$

Let

$$Y_i = \begin{cases} 1 & \text{if cell } i \text{ has a defect free flight} \\ 0 & \text{otherwise.} \end{cases}$$

Assuming the Y_i's are mutually independent random variables, $T = \sum_{i=1}^{n'} Y_i$ = number of cells operating satisfactorily at the end of the flight, and Y_i is a binomial random variable with parameters n' and q. A conservative rule for calculating n' would be to find the binomial distribution whose probability of being at least n (optimal value determined previously) is 0.90. This would provide assurance that a sufficient number of cells will remain operable. The p_i's can be estimated if results from similar experiments are available. If not, the experimenter may have to subjectively estimate the p_i's. At least conservative upper bounds for the p's can certainly be given.

Electron Irradiation In Space

Although the data from radiation effects on GaAs solar cells is limited, we will show how to predict degradation in a space environment due to electron irradiation. It must be emphasized that the cells tested in the laboratory were not radiation hardened and so the predictions made here will be underestimates for life expectancy in an actual space flight. The prediction equations are based upon deep junction cells which are expected to degrade rapidly.

From the laboratory data of solar cell degradation versus fluence analyzed earlier, we have obtained the prediction equation

$$\log\left(\frac{I_{sco}}{I_{sc}} - 1\right) = 0.8649 + 0.194x_j + 1.075 \log(\phi/10^{16}) \qquad (11)$$

where ϕ is the fluence [1 MeV e/cm^2] and x_j is the junction depth [μm]. For a 25 percent reduction in the short-circuit current $I_{sc}/I_{sco} = 0.75$, equation (11) can be expressed

$$\phi \doteq 10^{14.7516 - 0.1805x_j} \qquad (12)$$

We assume that $\phi = Qt$ where $Q = Q(E > 0.5)$ is the integrated flux of electrons with energies greater than 0.5 MeV, which has the dimensions [electrons/cm^2-sec]. Values of Q are obtained from figure 5, (from ref. 7) for various orbits. For synchronous orbits the altitude is between L = 5 and L = 7 earth radii and the flux Q varies between $5(10^6)$ and $2(10^6)$ electrons/cm^2-sec. Using the equation (12) with $x_j = 0.5$[μm], table 4 gives estimates for the predicted time t [days] for a solar cell to degrade by 25 percent.

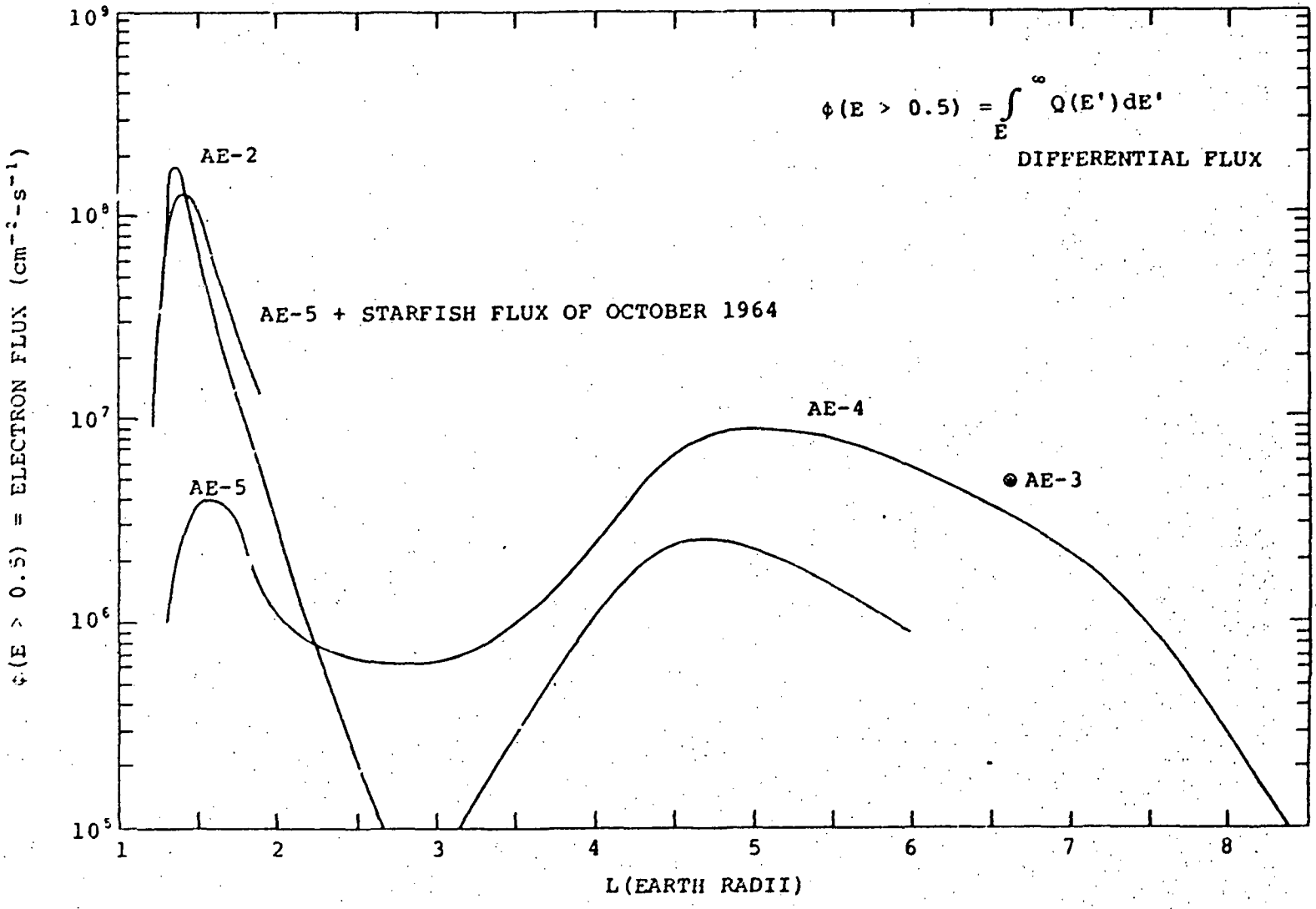

Figure 5. Radial profile of omnidirectional equatorial flux of electrons with energies above 0.5 MeV near solar minimum (taken from ref. 7).

Table 4. Time (days) for GaAs solar cell to degrade by 25 percent for a junction depth of 0.5.

Earth Radii	Electron Flux with Energies Above 0.5 MeV	Times (Days) to Degrade 25%
L	Q	t
5	$8(10^6)$	663
6	$5(10^6)$	1061
7	$2(10^6)$	2653

The values of t in table 4 are lower bounds on the expected time to degrade 25 percent and are based upon the prediction equation obtained from laboratory data on deep junction cells. This prediction equation does not take into account the temperature effects on the operating characteristics of the GaAs solar cell. GaAs solar cells can operate up to 300°C, and laboratory data is just now being obtained (ref. 8) which demonstrates that radiation damage caused by electrons can be removed with annealing. Thus, the predicted times to degrade by 25 percent are probably way too low. It is expected that with proper annealing of radiation damage encountered in an orbit there can be imposed a significant reduction in the expected radiation damage. However, further research into this important area is needed to verify this conjecture.

Summary

The completely randomized design previously discussed (see "Experimental Design") was chosen since only one source of variability (difference in treatments) was obvious. A one-way analysis of variance is then the appropriate first step in the analysis. If the experimenter so desires, the experiment could be considered as a two-factor experiment with factors (1) type of cell and (2) amount of annealing. A two-way analysis of variance would then be the first step in the analysis (ref. 6). The sample size discussion would be similar, however.

THEORETICAL CONSIDERATIONS

In order to augment the limited data on radiation damage to GaAs solar cells, a modeling approach is presented in order to compare theory and experimental results. This modeling approach consists of developing a mathematical model based upon the diffusion of holes and electrons within the various regions of the GaAs solar cell. The resulting model contains various physical parameters such as diffusion lengths, mobilities, recombination velocities, etc. It is assumed that the degradation in the electrical properties of a solar cell that has been exposed to an electron irradiation can be explained by determining the effect of the radiation on these parameters (i.e. degradation of device parameters).

Background Material

The following is a summary of existing models of semiconductor behavior (refs. 9 to 17). Consider the separate regions of p- and n-type semiconductor materials which are combined to form a junction as in figure 6. The n-type material has a large density of electrons, and the p-type material has a large density of holes. In the n-type material the electrons are referred to as majority carriers, and any holes created in the n-type material are referred to as minority carriers. In the p-type material the holes are the majority carriers and any electrons that are freed from bonds are called minority carriers. When the n- and p-type materials are combined there is a diffusion of holes from the p-region to the n-region, and simultaneously there is a diffusion of electrons from the n- to the p-region. This diffusion process continues until an equilibrium state has been achieved. As the electrons diffuse from n to p they leave behind donor ions N_d^+ in the n material, and holes diffusing from p to n leave behind acceptor ions N_a^-. Thus atoms on either side of the junction become ionized. The charge associated with an ionized atom is not free to move about within the crystal structure, and thus there is produced an electric field E which is directed from the positive charge toward the negative charge. This electric field E appears in some region W about the junction which

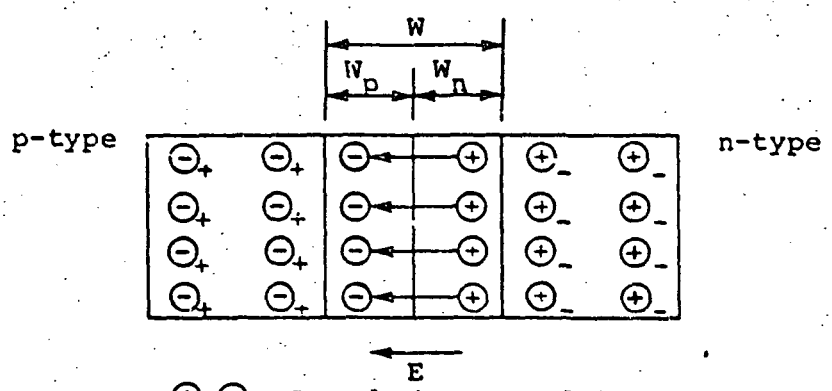

(a)

⊕, ⊖ = Bound charges of impurity atoms in n- and p-type material

+, - = Positive (holes), negative (electrons)

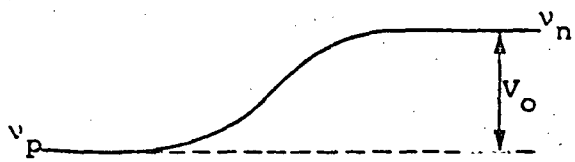

(b)

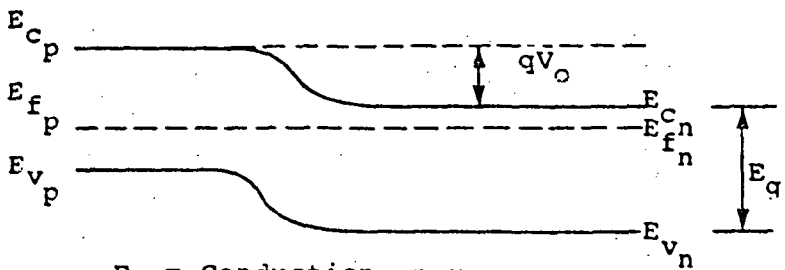

(c)

E_c = Conduction energy

E_v = Valence energy

E_f = Fermi level

Figure 6. (a) Depletion region, (b) electrostatic potential, and (c) energy band diagram of p- or n-type material.

is called the depletion or space charge region, and there is an equilibrium potential difference $V_o = \nu_n - \nu_p$ across the region W, where ν is the electrostatic potential and $-\frac{d\nu}{dx} = E$.

At equilibrium the drift and diffusion components of the hole current become balanced. Thus, letting J denote the current density, we have at equilibrium

$$J_p(x) = J_{drift} + J_{diffusion} = 0$$

$$J_p(x) = q\,\mu_p\,p(x)E - q\,D_p\,\frac{dp}{dx} = 0 \qquad (13)$$

where $p = p(x)$ = hole density [cm^{-3}]

D_p = diffusion coefficient [cm^2/sec]

μ_p = hole mobility [$cm^2/(volt\text{-}sec)$]

q = electron charge [coulomb]

The diffusion coefficient and mobility are related by the Einstein relation

$$D_p = \mu_p\,KT/q \qquad (14)$$

where K = Boltzman's constant. [J/°K] and T = temperature [°K]. From the equations (13) and (14) we obtain the integral

$$\frac{-q}{KT}\int_{\nu_p}^{\nu_n}\frac{d\nu}{dx}\,dx = \int_{p_p}^{p_n}\frac{1}{p}\,\frac{dp}{dx}\,dx$$

which gives

$$\frac{-q}{KT}\,(\nu_n - \nu_p) = \ell n\left(\frac{p_n}{p_p}\right) = \frac{-q}{KT}\,V_o \qquad (15)$$

where p_n, p_p, (n_n, n_p) are the equilibrium densities of holes (electrons) on either side of the junction. At equilibrium

$$N_a\, n_p = n_i^2 = p_n\, N_d \tag{16}$$

where n_i is called the intrinsic carrier density. If there are N_a acceptors on the p-side and N_d donors on the n-side we can write equation (15) as

$$V_o = \frac{KT}{q} \ln\left(\frac{N_a}{n_i^2/N_d}\right) = \frac{KT}{q} \ln\left(\frac{N_a N_d}{n_i^2}\right). \tag{17}$$

This is the theoretical maximum open-circuit voltage that can be achieved. From equations (15) and (16) we let

$$p_{n_o} = p_p e^{\frac{-qV_o}{KT}} \text{ and } n_{p_o} = n_n e^{\frac{-qV_o}{KT}}$$

where V_o is the theoretical maximum electrostatic potential difference across the depletion region and p_{n_o} denotes the value of p_n at $x = -W_p$ and n_{p_o} denotes the value of n_p at $x = -W_n$. We then have in terms of the actual potential difference $V_o - V$ across the junction that

$$p_n = p_p e^{\frac{-q(V_o - V)}{KT}} = p_{n_o}\, e^{qV/KT} \text{ and}$$

$$n_p = n_n e^{\frac{-q(V_o - V)}{KT}} = n_{p_o}\, e^{qV/KT} \tag{18}$$

The carrier density varies with temperature and band gap energy according to the relation

$$n_i = 2\left(\frac{2\pi KT}{h^2}\right)^{3/2} (M_n^* M_p^*)^{3/4}\, e^{-E_g/2KT} \tag{19}$$

where M_n^*, M_p^* are the effective masses of holes and electrons in the semiconductor material. For $M_n^* = M_e^*\, M_o$, $M_p^* = M_h^*\, M_o$, M_e^* 0.068, $M_h^* = 0.53$ and M_o = the mass of an electron, equation (19) can be written as

$$n_i^2 = (M_e^* M_h^*)^{3/2} (23.3172)(10^{30}) T^3 e^{-E_g/KT}$$

$$= 0.84(10^{30}) T^3 e^{-E_g/KT} \qquad (20)$$

where the band gap energy E_g, in electron volts, can be approximated by

$$E_g = 1.522 - \frac{5.8(10^{-4}) T^2}{T + 300}$$

$$E_g \cong 1.43 \text{ ev} \quad @ \; T = 300°K \qquad (21)$$

where T = temperature [°K], K = Boltzman's constant [eV/°K].

The width W of the depletion region is $W = W_p + W_n$ and can be determined by examining the charge density within the depletion region. At equilibrium we have

$$qAW_p N_a = qAW_n N_d \qquad (22)$$

where A is the cross-sectional area of the solar cell. Using Gauss's law, the gradient of the electric field can be related to the space charge at any point x about the center of the space charge region and we can write (see fig. 7):

$$\frac{dE}{dx} = \frac{q}{\varepsilon} N_d, \quad 0 \leq X \leq W_n$$

$$\frac{dE}{dx} = \frac{-q}{\varepsilon} N_a, \quad -W_p \leq X \leq 0 \qquad (23)$$

where $\varepsilon = \varepsilon_r \varepsilon_o$ is the permitivity of the material and $\varepsilon_o = 8.85(10^{-14})$ F/cm is the permitivity of free space (for GaAs $\varepsilon_r = 10.9$).

Integrating the equations (23) gives

$$E_o = \frac{-q}{\varepsilon} N_d W_n = \frac{-q}{\varepsilon} N_a W_p \qquad (24)$$

(a)

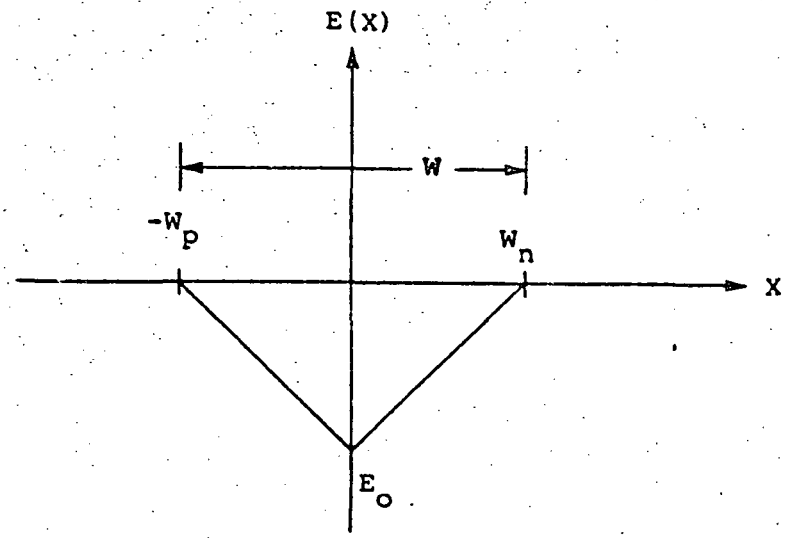

(b)

	HOLES	ELECTRONS	
	p_p	n_n	Majority carrier concentration [cm^{-3}]
	p_n	n_p	Minority carrier concentration [cm^{-3}]
	n_{p_o}	n_{p_o}	Minority carrier concentration at thermal equilibrium [cm^{-3}]
n-type donor	N_D	N_a p-type acceptor	Impurity concentration [cm^{-3}]

Figure 7. (a) Depletion region and (b) symbolism.

Now, $-V_o = \int_{-W_p}^{W_n} E(x)dx = \frac{1}{2} E_c W = -\frac{1}{2} \frac{q}{\varepsilon} N_d W_n W$

where $W = W_n + W_p$ and from equation (24) $N_d W_n = N_a W_p$ so that these equations can be combined to give

$$W^2 = \frac{2\varepsilon V_o}{q}\left(\frac{N_a + N_d}{N_a N_d}\right) \tag{25}$$

In the case of nonequilibrium where there is a voltage V applied, the altered value of the electrostatic potential is $V_o - V$ and equation (25) can be written

$$W^2 = \frac{2\varepsilon(V_o - V)}{q}\left(\frac{N_a + N_d}{N_a N_d}\right) \tag{26}$$

$Ga_{1-x}\ Al_xAs$ Solar Cell

With reference to figure 8, a model of a $Ga_{1-x}\ Al_xAs$ solar cell, the various processes of interest are that:

1. Some photons are reflected from the surface.

2. Photons with short wavelengths generate hole-electron pairs close to the surface of the cell. Some of these pairs quickly recombine, and others are injected into the p-GaAs region.

3. Photons generate hole-electron pairs in the p-GaAs. Here electrons move toward the depletion region and contribute to the short-circuit current at the junction edge.

4. Holes generated in the n-GaAs region diffuse toward junction and contribute to the short-circuit current.

Proceeding as in references 9 and 10, the following equations for the photocurrent can be developed. When incident photons have an energy greater than the band gap energy, absorption of the photons causes electrons to be raised in energy from the valence band E_v to the conduction band E_c creating hole-electron pairs. We will be concerned with excess minority carriers (holes on the n-side and electrons of the p-side) which diffuse to the edges of the depletion region before they recombine.

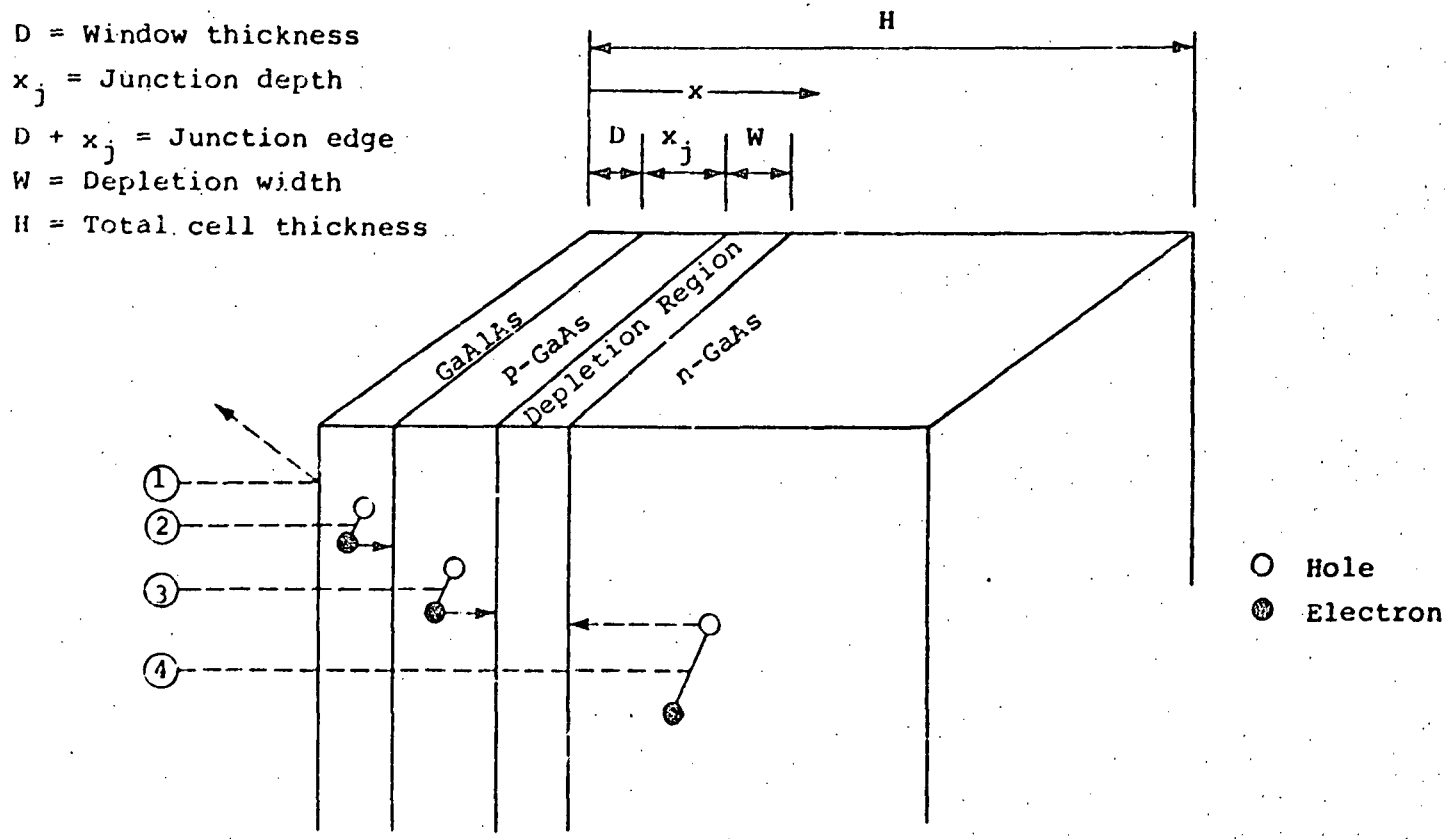

Figure 8. GaAlAs solar cell geometry.

It is these minority carriers which produce a photocurrent, photovoltage and consequently solar cell power. Let $p_n - p_{n_o}$ denote the excess hole density in the n-GaAs material and let $n_p - n_{p_o}$ denote the excess electron density in the p-GaAs material. At a surface, the minority carrier current density is given by $J_{surface}$, where $J_{surface} = qS_p\left(p_n - p_{n_o}\right)$ n-type material [amp/cm^2] $= qS_n\left(n_p - n_{p_o}\right)$ p-type material

with
q = electron (hole) charge [coulombs]
S_p = surface recombination velocity of holes [cm/sec]
S_n = surface recombination velocity of electrons [cm/sec]
$p_n - p_{n_c}$ = hole density [cm^{-3}]
$n_p - n_{p_o}$ = electron density [cm^{-3}]

Consider the hole flux per unit volume entering and leaving a volume element of the solar cell. We have

$$\frac{\partial}{\partial t}\left(p_n - p_{n_o}\right) = \lim_{\Delta x \to 0}\left[\frac{J(x) - J(x + \Delta x)}{q\Delta x}\right] - g_r + G_r$$

(rate of hole build-up) = (increase in hole density per unit time) − (recombination + (generation rate).
rate)

Where J is the current density of the holes. This gives the continuity equation for holes as

$$\frac{\partial p_n}{\partial t} = + \frac{1}{q}\frac{dJ_p}{dx} - g_r + G_r \qquad (27)$$

Similarly, the continuity equation for electrons is

$$\frac{\partial n_p}{\partial t} = \frac{-1}{q}\frac{dJ_n}{dx} - g_r + G_r \qquad (28)$$

Let β, α denote the absorption coefficients for the GaAlAs and GaAs regions respectively, then the generation rate for hole-electron pairs can be expressed as

$$G_a = \beta F_o (1 - R)\, e^{-\beta x},\quad 0 \leq x \leq D$$

$$G_g = \alpha F_o (1 - R)\, e^{-\beta D} e^{-\alpha (x-D)},\quad D \leq x \leq D + x_j$$

$$G_p = \alpha F_o (1 - R)\, e^{-\beta D} e^{-\alpha x_j} e^{-\alpha \left(x-(D+d)\right)},\quad D + x_j \leq x \leq H \qquad (29)$$

where R = fraction of light reflected from the surface of the solar cell and F_o = number of photons incident per square centimeter. The recombination rates in the various regions are expressed as

$$g_a = \left(\frac{n_p - n_{p_o}}{\tau_a}\right),\ \tau_a = \text{lifetime of an electron in GaAlAs}$$

$$g_g = \left(\frac{n_p - n_{p_o}}{\tau_g}\right),\ \tau_g = \text{lifetime of an electron in p-GaAs}$$

$$g_p = \left(\frac{p_n - p_{n_o}}{\tau_p}\right),\ \tau_p = \text{lifetime of a hole in n-GaAs} \qquad (30)$$

For steady-state conditions, the continuity equations for the different regions become:

For electrons in the p-type GaAlAs material

$$-\frac{1}{q}\frac{dJ_a}{dx} + G_a - \left(\frac{n_p - n_{p_o}}{\tau_a}\right) = 0 \qquad (31a)$$

For electrons in the p-type GaAs material

$$-\frac{1}{q}\frac{dJ_g}{dx} + G_g - \left(\frac{n_p - n_{p_o}}{\tau_g}\right) = 0 \qquad (31b)$$

For holes in the n-type GaAs material

$$\frac{1}{q}\frac{dJ_p}{dx} + G_p - \left(\frac{p_n - p_{n_o}}{\tau_p}\right) = 0 \qquad (31c)$$

where $-\frac{1}{q}\frac{dJ}{dx}$ = divergence of current = increase in electron (hole) density per unit volume per unit time, and G = generation rate.

The hole and electron diffusion currents in these regions are

$$J_a = -q D_a \frac{d}{dx}\left(n_p - n_{p_o}\right) \qquad (32a)$$

$$J_g = -q D_g \frac{d}{dx}\left(n_p - n_{p_c}\right) \qquad (32b)$$

$$J_p = q D_p \frac{d}{dx}\left(p_n - p_{n_o}\right) \qquad (32c)$$

where D_a, D_g, D_p are the diffusion coefficients for the GaAlAs, p-GaAs and n-GaAs regions, denoted by the subscripts a, g and p.

From equations (31a) and (32a) we obtain the diffusion equation for the GaAlAs region as

$$D_a \frac{d^2\left(n_p - n_{p_o}\right)}{dx^2} - \frac{\left(n_p - n_{p_o}\right)}{\tau_a} + \beta(1 - R)F_o e^{-\beta x} = 0, \quad 0 \leq x \leq D$$

which is subject to the boundary conditions

$$q S_a\left(n_p - n_{p_o}\right) = q D_a \frac{d}{dx}\left(n_p - n_{p_o}\right) \text{ at } x = 0$$

and

$$n_p - n_{p_o} = 0 \quad \text{at } x = D. \qquad (33)$$

After solving equation (33) the photocurrent contribution at X = D is given by

$$J_D = - q D_a \frac{d}{dx}\left(n_p - n_{p_o}\right)\Big|_{x=D} \tag{34}$$

which is injected into the p-GaAs region at the interface. Solving equation (33) and calculating equation (34) gives this current in the form

$$J_D = \frac{-qF_o(1 - R)\beta L_a}{\beta^2 L_a^2 - 1}\left[\beta L_a e^{-\beta D} + f_1\right] \tag{35}$$

where

$$f_1 = \frac{e^{-\beta D}\left[\sinh\left(\frac{D}{L_a}\right) + \frac{\tau_a S_a}{L_a}\cosh\left(\frac{D}{L_a}\right)\right] - \beta L_a - \frac{\tau_a S_a}{L_a}}{\frac{\tau_a S_a}{L_a}\sinh\left(\frac{D}{L_a}\right) + \cosh\left(\frac{D}{L_a}\right)} \tag{36}$$

and $L_a = \sqrt{D_a \tau_a}$ = diffusion length in GaAlAs.

For the p-GaAs region, we have from equations (31b) and (32b) the diffusion equation

$$D_g \frac{d^2\left(n_p - n_{p_o}\right)}{dx^2} - \frac{\left(n_p - n_{p_o}\right)}{\tau_g} + \alpha F_o(1 - R)e^{-\beta D}e^{-\alpha(x-D)} = 0,$$

$$D \leq x \leq D + x_j \tag{37}$$

which is subject to the boundary conditions

$$S_g\left(n_p - n_{p_o}\right) - \frac{J_D}{q} = D_g \frac{d}{dx}\left(n_p - n_{p_o}\right) \text{ at } x = D$$

and

$$\left(n_p - n_{p_o}\right) = 0 \quad \text{at } x = D + x_j \tag{38}$$

From the solution of equation (37) the photocurrent at $x = D + x_j$ is given by

$$J_{D+x_j} = - qD_g \frac{d}{dx}\left(n_p - n_{p_o}\right)\Big|_{x = D + x_j} \tag{38}$$

Solving equation (37) and calculating equation (38) gives

$$J_{D+x_j} = \frac{-qF_o(1 - R)\alpha L_g e^{-\beta D}}{\alpha^2 L_g^2 - 1}\left[\frac{f_2}{f_3} + \alpha L_g e^{-\alpha x_j}\right] + \frac{J_D}{f_3} \tag{39}$$

where

$$f_2 = e^{-\alpha x_j}\left\{\sinh\left(\frac{x_j}{L_g}\right) + \frac{S_g\tau_g}{L_g}\cosh\left(\frac{x_j}{L_g}\right)\right\} - \alpha L_g - \frac{\tau_g S_g}{L_g} \tag{40}$$

$$f_3 = \frac{S_g\tau_g}{L_g}\sinh\left(\frac{x_j}{L_g}\right) + \cosh\left(\frac{x_j}{L_g}\right) \tag{41}$$

and

$$L_g = \sqrt{D_g\tau_g} = \text{diffusion length in p-GaAs}$$

For the base region, equations (31c) and (32c) give the diffusion equation

$$D_p \frac{d^2\left(p_n - p_{n_o}\right)}{dx^2} - \frac{\left(p_n - p_{n_o}\right)}{\tau_p} + \alpha F_o(1 - R)e^{-\beta D}e^{-\alpha x_j}e^{-\alpha\left(x-(D+x_j)\right)}$$

$$= 0, \quad D + x_j + W \leq x \leq H$$

which is subject to the boundary conditions

$$p_n - p_{n_o} = 0 \quad \text{at } x = D + x_j + W$$

$$S_p\left(p_n - p_{n_o}\right) = -D_p \frac{d}{dx}\left(p_n - p_{n_o}\right) \text{ at } x = H. \tag{42}$$

Solution of equation (42) gives the photocurrent at $x = D + x_j + W$ as

$$J_{D + x_j + W} = qD_p \frac{d}{dx}\left(p_n - p_{n_o}\right)\Big|_{x=D+x_j+W} \tag{43}$$

We calculate this current to be

$$J_{D+x_j+W} = \frac{qF_o(1 - R)\alpha L_p e^{-\beta D} e^{-\alpha x_j} e^{-\alpha W}}{\alpha^2 L_p^2 - 1} [\ldots_p - f_4] \tag{44}$$

where

$$f_4 = \frac{\sinh\left(\frac{H^*}{L_p}\right) + \alpha L_p e^{-\alpha H^*} + \frac{S_p L_p}{D_p}\left\{\cosh\left(\frac{H^*}{L_p}\right) - e^{-\alpha H^*}\right\}}{\frac{S_p L_p}{D_p}\sinh\left(\frac{H^*}{L_p}\right) + \cosh\left(\frac{H^*}{L_p}\right)}$$

$$L_p = \sqrt{D_p \tau_p} \quad \text{and} \quad H^* = H - (D + x_j + W). \tag{45}$$

For large S_p we have $\lim_{S_p \to \infty} f_4 = 1$ and equation (45) reduces to

$$J_{D + x_j + W} = \frac{qF_o(1 - R)\alpha L_p e^{-\beta D} e^{-\alpha x_j} e^{-\alpha W}}{\alpha L_p + 1} \tag{46}$$

Equations (35) and (39) have removable singularities where $\beta^2 L_a^2 = 1$ and $\alpha^2 L_g^2 = 1$ respectively. Introducing the functions

$$f(x,y) = \begin{cases} -y/2 & , x = 1 \\ \frac{-y}{2u} e^u \sinh(u), & x \neq 1, \; u = \frac{y(1 - x)}{2} \end{cases} \tag{47}$$

and

$$F(x,y,z) = \frac{-qF_o(1 - R)x}{y \sinh z + \cosh z}\left\{(y + 1)\left[f(x,z) + \frac{1/2}{x + 1}\right]\right.$$

$$\left. + \frac{1}{x + 1}\left[\frac{(1 - y)}{2} e^{-z(1+x)} - 1\right]\right\} \qquad (48)$$

Equations (35) and (39) can be represented in the alternate forms

$$J_D = F\left(\beta L_a, \frac{\tau_a S_a}{L_a}, \frac{D}{L_a}\right) \qquad (49)$$

and

$$J_{D+x_j} = F\left(\alpha L_g, \frac{\tau_g S_g}{L_g}, \frac{x_j}{L_g}\right) + J_D \Big/ \left(\frac{\tau_g S_g}{L_g} \sinh\left(\frac{x_j}{L_g}\right) + \cosh\left(\frac{x_j}{L_g}\right)\right) \qquad (50)$$

Some photocurrent collection also occurs in the depletion region. If the electric field in this region is high enough, then the minority carriers will be accelerated out of the region before they can recombine. The photocurrent contribution from this type of excitation is simply the number of photons absorbed and is given by

$$J_W = \text{photon density entering} - \text{photon density leaving}$$

$$J_W = qF_o(1 - R)e^{-\beta D}e^{-\alpha x_j}[1 - e^{-\alpha W}] \qquad (51)$$

The total photocurrent is the sum of the photocurrents given by equations (46), (50), and (51) and is denoted by J_p. We have

$$J_p(\lambda) = J_{D+x_j}(\lambda) + J_{D+x_j+W}(\lambda) + J_W(\lambda) \qquad (52)$$

Spectral Response-Short-Circuit Current

The spectral response of the solar cell is a function of wavelength and is given by

$$SR(\lambda) = \frac{J_p(\lambda)}{qF_o(1 - R)} \tag{53}$$

where in equation (52) the absorption coefficients α and β are functions of wavelength λ[microns] and ρ the percentage of Al in $Ga_{1-\rho}Al_{\rho}As$. These absorption coefficients are approximated by the relations:

$$\alpha = \left\{ \begin{array}{ll} 0 & , E \leq 1.38 \\ 5.5074(10^4)\sqrt{E - 1.3779}/E, & 1.38 < E \leq 1.50 \\ 1.2824(10^4)\ (E - 0.5)^{2.5} & , 1.50 \leq E \end{array} \right\} \tag{54}$$

and

$$\beta = \left\{ \begin{array}{ll} 0 & E < E_1 = 1.38 + 0.9535\rho \\ f_1(E), & E_1 < E \leq E_2 = 1.5 + 1.4535\rho \\ f_2(E), & E_2 \leq E \end{array} \right\} \tag{55}$$

where $E = 1.2402/\lambda$ is the photon energy [eV] at wavelength λ[microns] and

$$f_2(E) = \left(1 - \frac{(\beta_{lim})(\rho)(E_2)}{E}\right)\left(1.2824(10^4)\right)(E - 0.5)^{2.5} \tag{56a}$$

and

$$f_1(E) = 10\ \exp\{K_1(E - E_1)\} + 523\rho\ \sin\left[\frac{(E - E_1)\pi}{E_2 - E_1}\right] \tag{56b}$$

with

$$K_1 = \frac{1}{(E_2 - E_1)}\ \ell n\left(\frac{f_2(E_2)}{10}\right).$$

The absorption coefficients α and β are illustrated in figure (9) for various values of the percentage of aluminum ρ. The parameter β_{lim} raises (β_{lim} near 1) and lowers (β_{lim} near 0.25) the GaAlAs absorption curve. For this study $\beta_{lim} = 0.75$.

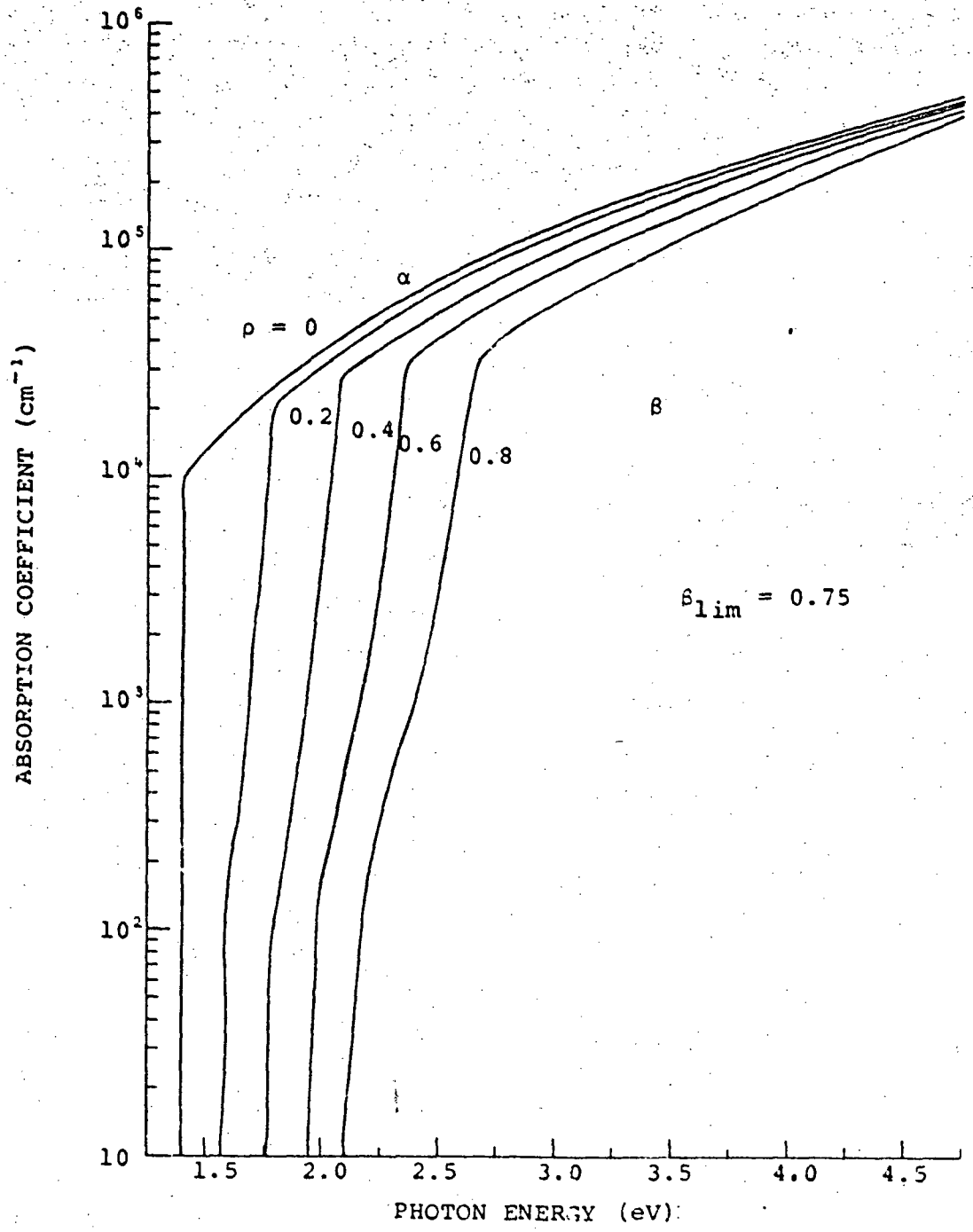

Figure 9. Absorption coefficient curves for $Ga_{1-p}Al_pAs$ for ρ = 0, 0.2, 0.4, 0.6 and 0.8.

The photocurrent at each wavelength λ [microns] is given by

$$J_p(\lambda) = qF_o(1 - R)SR(\lambda) \tag{57}$$

and the total photocurrent contributed from all wavelengths greater than or equal to λ_1 is the continuous sum given by

$$J_{sc} = q\int_{\lambda_1}^{\infty} F_o(1 - R)SR(\lambda)d\lambda \tag{58}$$

which may also be expressed in the form

$$J_{sc} = \frac{q}{hc}\int_{\lambda_1}^{\infty} (1 - R)p(\lambda) \cdot\lambda\cdot SR(\lambda)d\lambda \tag{59}$$

where h = Planck's constant, c = speed of light, and $p(\lambda)$ [$Wcm^{-2}\mu m^{-1}$] is the average solar spectral irradiance at 1.A.U. which has a solar constant of 135.3[$mW\cdot cm^{-2}$]. Values of $p(\lambda)$ can be found in references 10 and 11.

The magnitude of the short-circuit current density at wavelength λ is given by equation (58) and is

$$J_{sc}(\lambda) = J_p = J_{D+x_j} + J_{D+x_j+W} + J_W \tag{60}$$

If there were no losses by reflection or recombination the maximum current density would be

$$J_{sc',\,max} = qF_o \tag{61}$$

Hence, the collection efficiency or quantum efficiency $Q(\lambda)$ is given by

$$Q(\lambda) = \frac{J_{sc}}{J_{sc',\,max}} = \frac{J_{D+x_j} + J_{D+x_j} + W + J_W}{qF_o} \tag{62}$$

The short-circuit current density can be expressed in terms of the quantum efficiency by the relation

$$J_{sc} = q \int_{\lambda_1}^{\infty} F_o Q(\lambda) d\lambda \tag{63}$$

Injected Currents and Recombination Currents

For the dark current associated with the solar cell we have:

(i) Electrons from the n-side injected to the p-side

$$-\frac{1}{q}\frac{dJ_n}{dx} - \frac{\left(n_p - n_{p_o}\right)}{\tau_g} = 0 \tag{64}$$

(ii) Holes from the p-side injected to the n-side

$$\frac{1}{q}\frac{dJ_p}{dx} - \frac{\left(p_n - p_{n_o}\right)}{\tau_g} = 0 \tag{65}$$

We also have the current equations

$$J_n = -qD_g \frac{d}{dx}\left(n_p - n_{p_o}\right) \tag{66}$$

$$J_p = qD_p \frac{d}{dx}\left(p_n - p_{n_o}\right) \tag{67}$$

Equations (64) and (66) produce the diffusion equation

$$D_g \frac{d^2}{dx^2}\left(n_p - n_{p_o}\right) - \frac{\left(n_p - n_{p_o}\right)}{\tau_g} = 0, \quad D \leq x \leq D + x_j$$

which is subject to the boundary conditions

$$n_p = n_{p_o} e^{\frac{qV}{KT}} \quad \text{at} \quad x = D + x_j$$

and

$$S_g\left(n_p - n_{p_o}\right) = D_g \frac{d}{dx}\left(n_p - n_{p_o}\right) \quad \text{at} \quad x = D \tag{68}$$

Equations (65) and (67) produce the diffusion equation

$$D_p \frac{d^2}{dx^2}\left(p_n - p_{n_o}\right) - \frac{\left(p_n - p_{n_o}\right)}{\tau_p} = 0, \quad D + x_j + W \leq x \leq H$$

which is subject to the boundary conditions

$$p_n = p_{n_o} e^{qV/KT} \text{ at } x = D + x_j + W$$

and

$$S_p\left(p_n - p_{n_o}\right) = -D_p \frac{d}{dx}\left(p_n - p_{n_o}\right) \text{ at } x = H \tag{69}$$

From equations (68) and (69) the injection current is given by

$$J_{inj} = qD_p \frac{d}{dx}\left(p_n - p_{n_o}\right)\Big|_{x=D+x_j+W} + qD_g \frac{d}{dx}\left(n_p - n_{p_o}\right)\Big|_{x=D+x_j} \tag{70}$$

Solving equations (68) and (69) produces the injection current

$$J_{inj} = J_o\left[e^{qV/KT} - 1\right] \tag{71}$$

where

$$J_o = G\left(\frac{qD_g n_i^2}{L_g N_a}, \frac{d}{L_g}, \frac{S_g L_g}{D_g}\right) + G\left(\frac{qD_p n_i^2}{L_p N_d}, \frac{H - (D + x_j + W)}{L_p}, \frac{S_p L_p}{D_p}\right) \tag{72}$$

with $G = G(\xi, \eta, \tau)$ given by

$$G(\xi, \eta, \tau) = \xi\left[\frac{\sinh(\eta) + \tau \cosh(\eta)}{\tau \sinh(\eta) + \cosh(\eta)}\right] \tag{73}$$

The recombination current in the depletion region has the maximum value given by (ref. 10):

$$J_{rec} = \frac{\pi n_i WKT}{\sqrt{\tau_p \tau_g}} \frac{\sinh\left(\frac{qV}{2KT}\right)}{(V_o - V)} \tag{74}$$

where V_o is given by equation (17) and W is obtained from equation (26).

The total current is then given by

$$J = J_{sc} - J_{inj} - J_{rec} \tag{75}$$

The open-circuit voltage is obtained from equations (59), (71), (74) and (75) by setting $J = 0$ in equation (75) and solving for the voltage $V = V_{oc}$. The power output of the solar cell is given by

$$p = JV \tag{76}$$

where J is obtained from equation (75) and at maximum power $V = V_{max}$, $J = J_{max}$, $p = p_{max}$. The voltage at maximum power can be obtained by solving the equation

$$\frac{dp}{dV} = J + V\frac{dJ}{dV} = 0 \tag{77}$$

for the voltage, $V = V_{max}$.

The efficiency of the solar cell is given by

$$EFF = \eta = \frac{p_{max} A_a}{p_{in} A_t} = \frac{p_{max} A_a}{(135.3)A_t} \tag{78}$$

where A_t is the total area of the solar cell and A_a is the actual area which equals the total area minus the finger area. The fill factor is calculated from the relation

$$FF = \frac{J_{max} V_{max}}{J_{sc} V_{oc}} \tag{79}$$

ANALYSIS OF DEVICE EQUATIONS AND COMPARISON WITH EXPERIMENTAL DATA

A computer program was written which incorporates the equations describing the solar cell behavior. In this program the spectral response as determined by equation (53) was treated as a function of variables L_a, S_a, L_g, S_g, μ_n and L_p. In addition, the mobility μ_n, μ_p of the minority carriers in the p-region and n-region are related to the diffusion constants of these regions by the Einstein relations

$$D_g = \mu_n \frac{KT}{q} \quad \text{and} \quad D_p = \mu_p \frac{KT}{q} \tag{80}$$

The diffusion lengths L_a, L_g, L_p, the diffusion constants D_a, D_g, D_p, and lifetimes τ_a, τ_g, τ_p in the respective regions GaAlAs, p-GaAs, and n-GaAs are related by

$$L_i^2 = D_i \tau_i \quad (i = a,g \text{ or } p) \tag{81}$$

The "other" parameters occurring in the equations which model the solar cell response were assigned the nominal values which are given in table 5.

The measured values of the spectral responses for each cell were normalized and compared with normalized values of the predicted spectral responses. Measured values of the open-circuit voltage and short-circuit current were also compared with the predicted values from the model. In particular, a Marquardt optimization algorithm was employed and the computer was asked to choose values of the parameters L_a, S_a, S_g, μ_n, L_p which would minimize the sums of squares errors as well as minimizing the absolute values of the following percent errors:

$$f_i(x_i) = \text{Error } (i) = \left[\frac{SR(\lambda_i) \text{ measured} - SR(\lambda_i) \text{ predicted}}{SR(\lambda_i) \text{ predicted}}\right] (100), \; i = 1, \ldots, 9 \tag{82}$$

(cont'd)

Table 5. Nominal values assigned to GaAs solar cell parameters (before irradiation values).

$L_a = 2.4(10^{-6})$ cm

$L_g = 3(10^{-4})$ cm

$L_p = 3(10^{-4})$ cm

$N_a = (10^{19})$

$N_d = 1.3(10^{17})$

$D = 0.4(10^{-4})$ cm

$X_j = 1.5(10^{-4})$ cm and $4.0(10^{-4})$ cm

$S_a = 10^6$ cm/sec

$S_g = 10^4$ cm/sec

ρ = 0.83% aluminum

$\mu_p = 300$

$\mu_n = 3300$

$T = 300$

$\tau_a = 1.0(10^{-9})$

$$f_{10}(x_i) = \text{Error (10)} = \left[\frac{V_{oc}\ \text{measured} - V_{oc}\ \text{predicted}}{V_{oc}\ \text{predicted}}\right] (100)$$

$$f_{11}(x_i) = \text{Error (11)} = \left[\frac{J_{sc}\ \text{measured} - J_{sc}\ \text{predicted}}{J_{sc}\ \text{predicted}}\right] (100) \quad (82)\ \text{(concl'd)}$$

where $\lambda_i (i = 1,\ldots,9)$ were the wavelengths 0.45 to 0.85 in steps of 0.05 microns. In the computer program, the variables $x_i (i = 1, \ldots, 6) = (L_a, S_a, S_g, \mu_n, L_p)$ were restricted to lie within certain regions $x_{imin} \leq x_i \leq x_{imax}$. This was accomplished by introducing the dummy variables $u_i (i = 1,\ldots, 6)$ which were related to x_i by the relations

$$x_i = \left(\frac{x_{imax} + x_{imin}}{2}\right) + \left(\frac{x_{imax} - x_{imin}}{2}\right) \tanh(u_i) \quad i = 1,\ldots, 6 \quad (83)$$

The variables $u_i (i = 1,\ldots, 6)$ were then allowed to vary over the range $-\infty < u_i < \infty$.

The Marguardt procedure utilized can be represented by the vector equation

$$\{x\}^{K+1} = \{x^K\} - \left[J^T(x^K)J(x^K) + \lambda_K I\right]^{-1} J^T(x^K)F(x^K)$$

where

$$F(x^K) = \left\{\text{Col}(f_1(x_i), f_2(x_i), \ldots, f_{12}(x_i)\right\}^K$$

$J(x^K)$ is the Jacobian evaluated at $\{x\}^K$, and λ_K is a parameter, usually 1, where $\lambda_K < 1$ represents a Newton type of iteration and $\lambda_K > 1$ represents a gradient type of iteration.

The device equations describing the behavior of a GaAlAs solar cell were able to fit the uniradiated data, and typical results are illustrated in table 6.

Table 6. Typical results from device equations.

CELL = 35B FLU = 0

KG = 0 KP = 0

SA = 1488265 SG = 16047.07

D = 4.000000000E-5 DL = 0.0004

MUP = 300 MUN = 3373.184

ND = 1.300000000E17 NA = 1.000000000E19

LA = 9.000000000E-6 LG = 0.0002764919 LP = 0.0005966502

XP = 0.8341 Blim = 0.75

TA = 1.000000000E-9 TG = 8.775881867E-10 TP = 4.594987145E-8

DA = 0.081 DG = 87.11121221 DP = 7.747387532

W = 1.118912755E-5 NI = 4246987.371

SF1 = 0.643F2 = 0.4751846961

WAVELENGTH	MEAS RESP	PRED RESP	PERCENT ERROR
0.4500	0.1700	0.1879	9.5059
0.5000	0.5400	0.5518	2.1438
0.5500	0.5700	0.5751	0.8938
0.6000	0.5800	0.5821	0.3565
0.6500	0.5700	0.5864	2.8010
0.7000	0.5900	0.5932	0.5351
0.7500	0.6100	0.6035	-1.0755
0.8000	0.6100	0.6188	1.4211
0.8500	0.6400	0.6400	0.0000

SUM OF ERRORS SQUARED = 107.1916172

VOPEN2

JSC = 14.1531103

VOC = 0.9859651972

When the computer was asked to minimize errors between the predicted and measured values for the irradiated solar cell data, usually one or more of the variables x_i moved to a boundary limit x_{imax} or x_{imin}, and so a separate analysis was performed on the data by letting only one variable change at a time.

Figures 10, 11, and 12 illustrate the typical spectral response curves before irradiation and after irradiating the solar cells with 10^{16} electrons/cm^2. Note that the after irradiation spectral response has been greatly reduced in the blue region (i.e. reduced more than that at the band edge). This reduction can be partially explained by a reduction of the minority carrier diffusion length L_g in the p-GaAs region. Figures 5, 6, and 7 illustrate the curves which result by changing the diffusion length parameter L_g and holding all the other parameter values fixed. The effect that the changing of the diffusion length L_g has on the spectral response at a fixed wavelength is illustrated in figure 13. Note that the change in the diffusion length parameter L_g explains the reduced spectral response in the red region, but a change in at least one additional parameter will be needed to explain the reduced spectral response in the blue region.

Candidates for the additional parameter change to explain the reduced blue response are the parameters S_g = recombination velocity and μ_n = mobility. These parameter changes and their effects on the spectral response curve are illustrated in figures 14, 15, and 16. Figure 16 shows the change in the spectral response at a fixed wavelength as the mobility changes from 3300 cm^2/volt-sec to 5 cm^2/volt-sec with the diffusion length held constant. This type of a reduction in the mobility is not realistic, and the change in the spectral response is not large enough to explain the overall reduced blue response. Consequently, the mobility parameter was ruled out.

The recombination velocity S_g at the p-GaAlAs, p-GaAs interface was varied, and the corresponding spectral response curves at a fixed wavelength are illustrated in figures 14 and 15. Those curves are for various fixed values of L_g. Computed

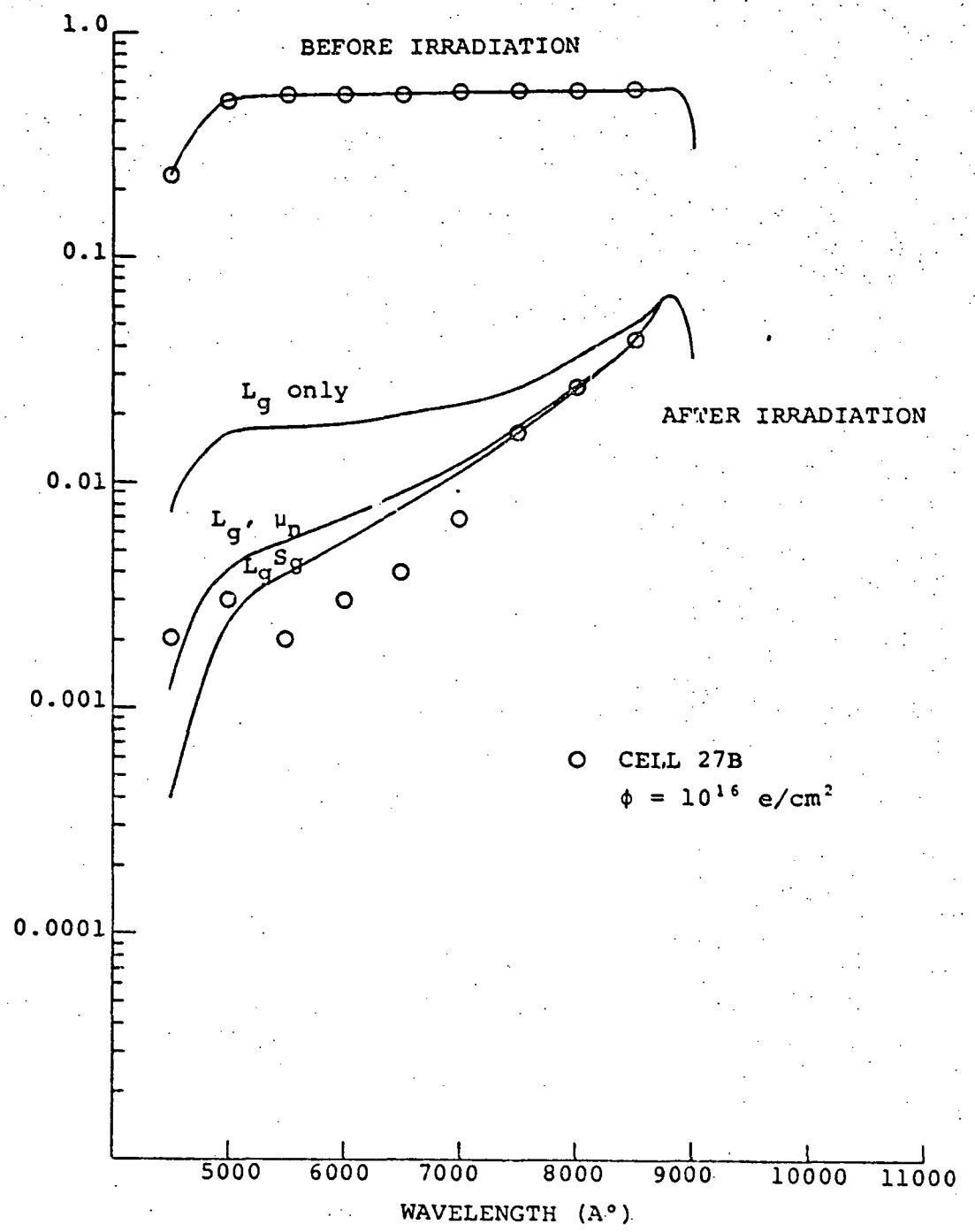

Figure 10. Spectral response curves before and after irradiation with 10^{16} electrons/cm^2.

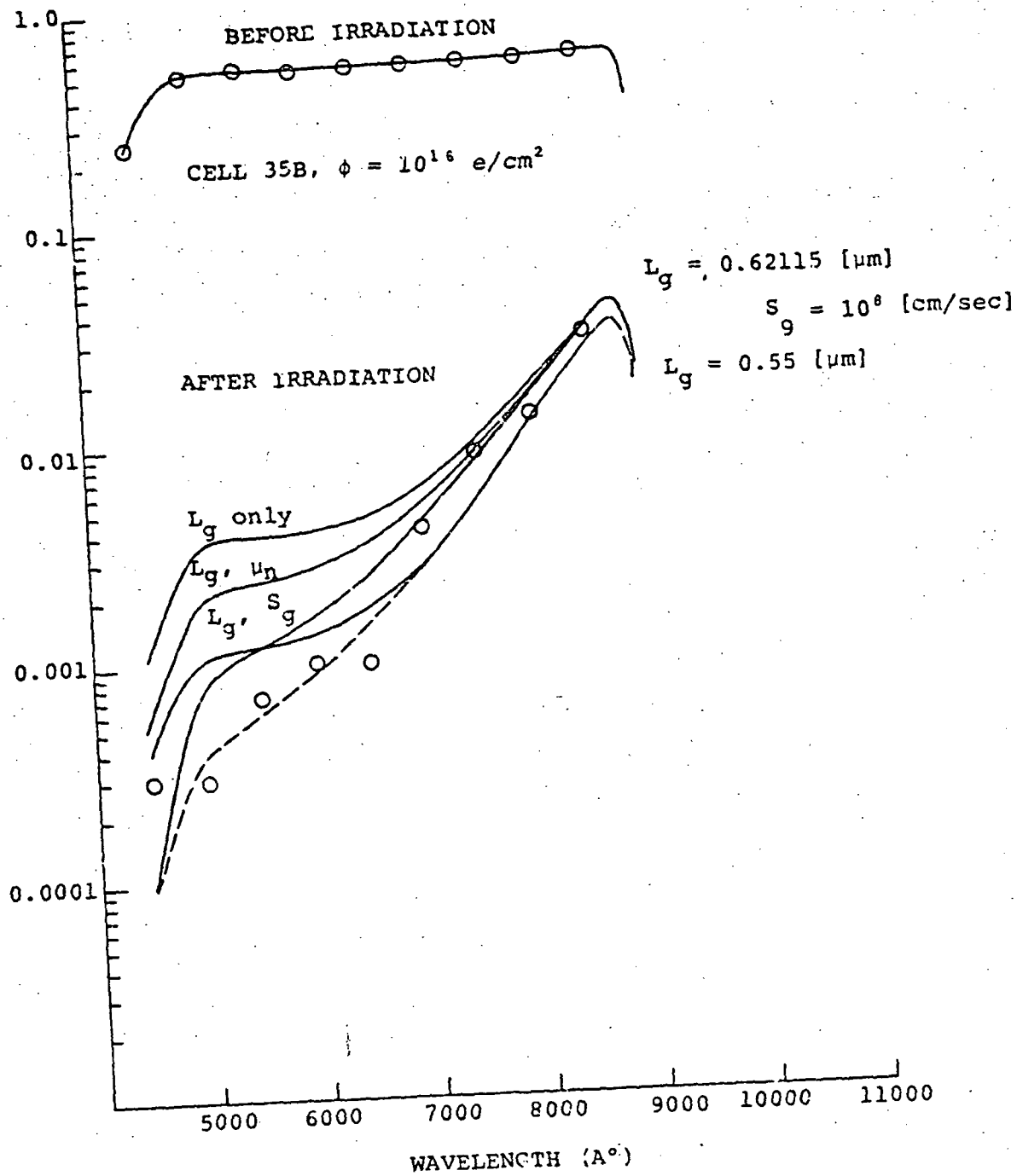

Figure 11. Spectral response curves before and after irradiation with 10^{16} electrons/cm^2.

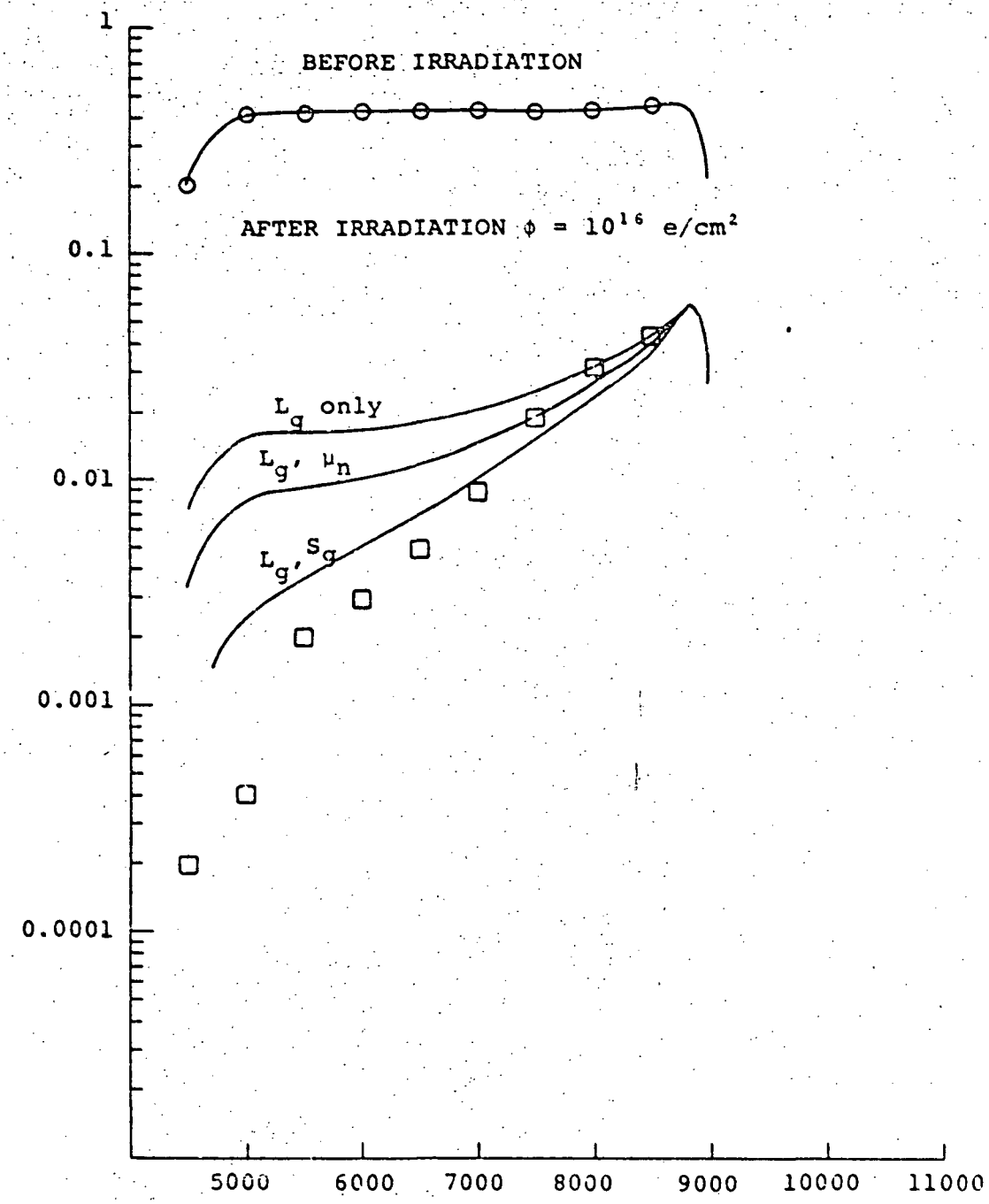

Figure 12. Before and after spectral response curves with L_g changing, L_g, μ_n changing, and L_g, S_g changing.

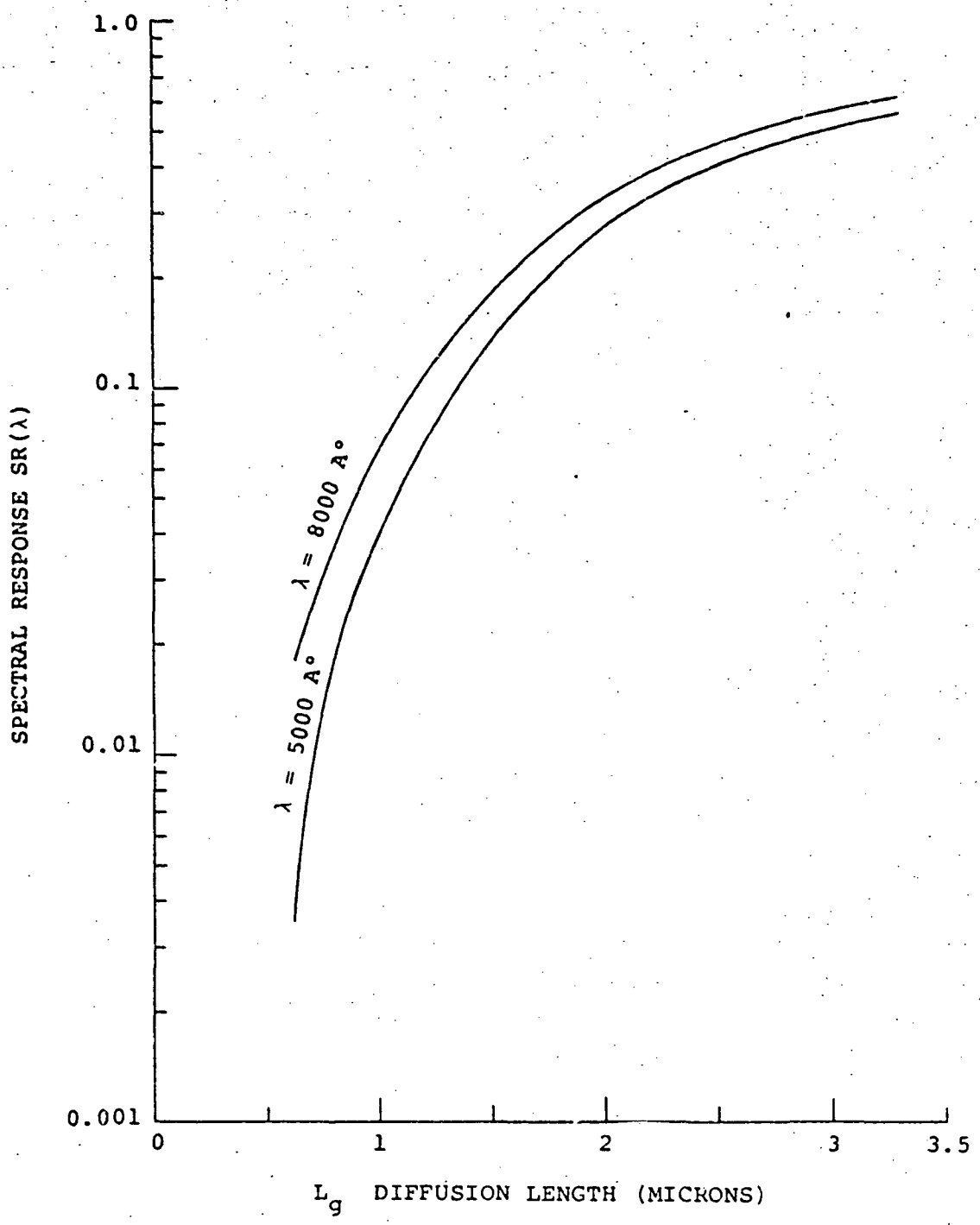

Figure 13. Spectral response at fixed wavelengths vs. diffusion length.

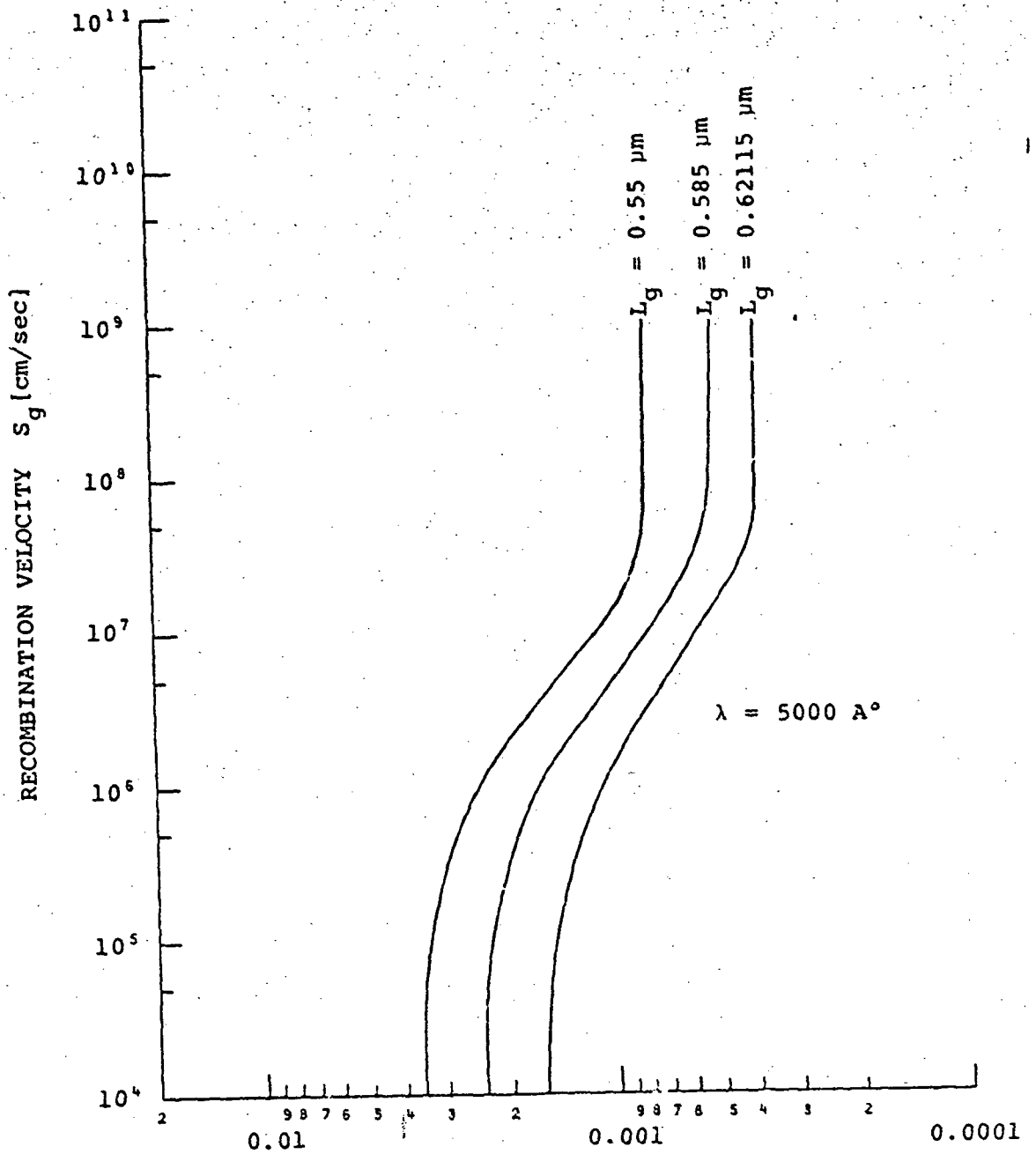

Figure 14. Spectral response SR(λ) at wavelength λ = 5000 A° for various values of diffusion length.

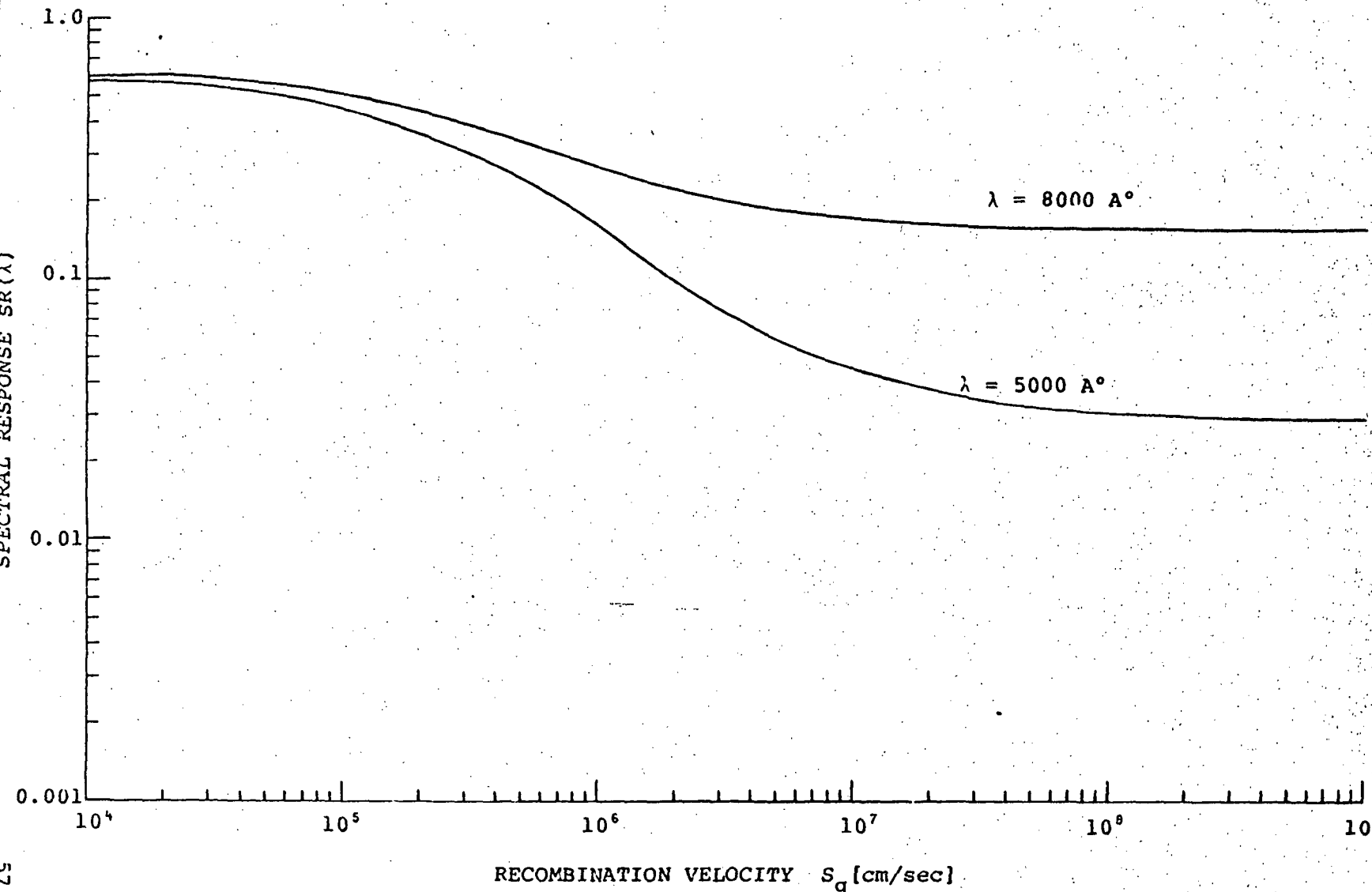

Figure 15. Spectral response vs. recombination velocity at wavelengths of 5000 and 8000 A°.

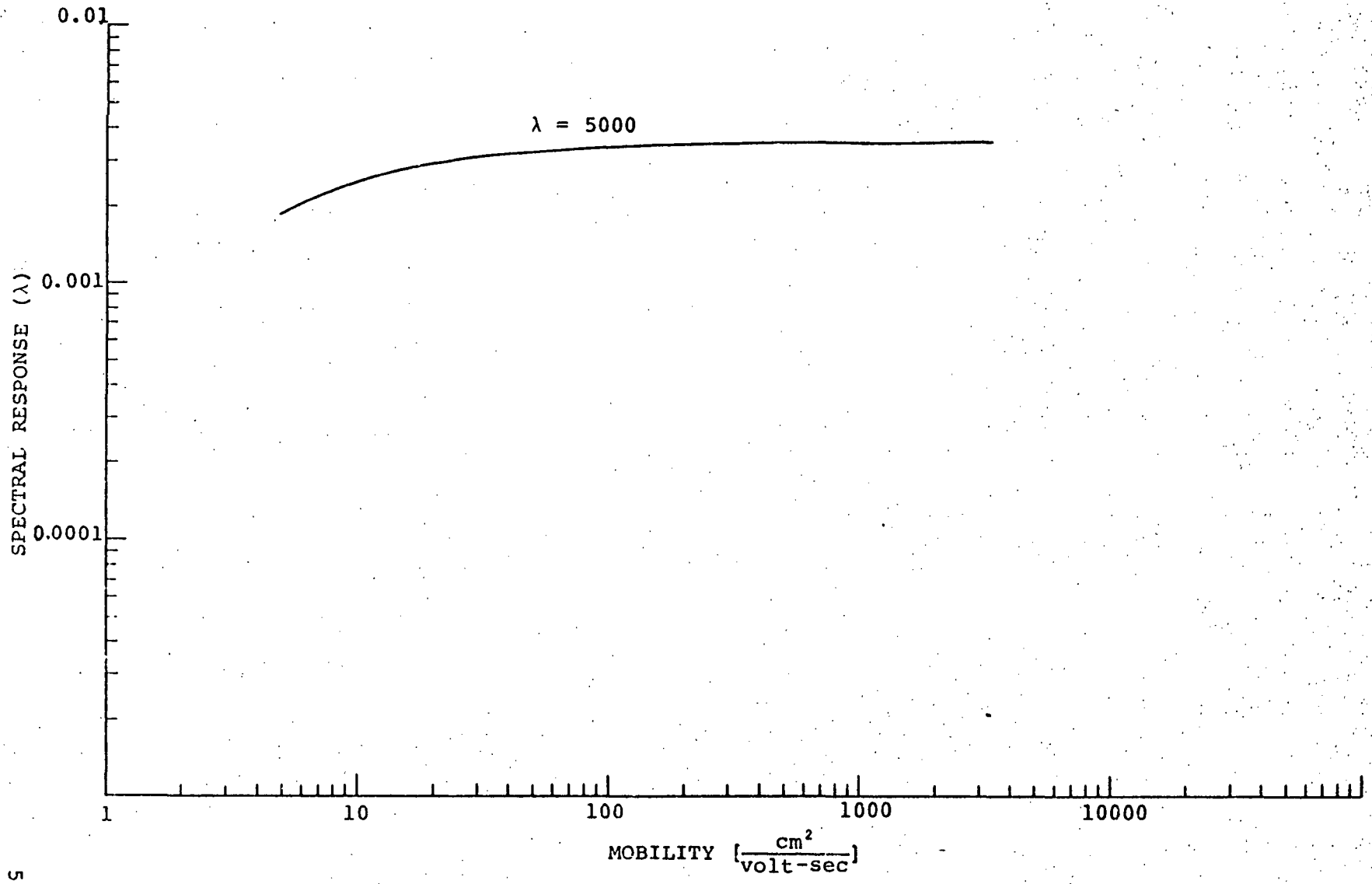

Figure 16. Spectral response vs. mobility at 5000 A°.

spectral response curves using values of S_g higher than the before irradiation values are also illustrated in figures 10, 11 and 12. Note that these changes in S_g will reduce the blue response and not greatly effect the spectral response in the red region.

The computer analysis of these parameter changes affected by 1 MeV electron irradiation resulted in the paper (ref. 18). A summary of the results in that paper is that the changes in the interface recombination velocity have been shown to be related to changes in the diffusion length produced by electron irradiation. These changes can be expressed

$$S_g = S_{go}\left(\frac{L_{g_o}}{L_g}\right)^2 \tag{84}$$

where the subscript o denotes initial values of the parameters before electron irradiation and S_g, L_g are values of the recombination velocity and diffusion length respectively after irradiation.

Model for Radiation Damage

Using the device equations developed in the previous sections, the computed spectral response curves can be made to agree with the experimental data by assuming a change in the minority carrier diffusion length given by (ref. 12):

$$\frac{1}{L_g^2} = \frac{1}{L_{g_o}^2} + K_g \phi \tag{85}$$

where L_{g_o} is the initial diffusion length (cm), L_g is the final diffusion length (cm), ϕ is the electron fluence (e/cm^2), and K_g is a damage coefficient. This type of change in the minority carrier diffusion length will account for the reduced spectral response in the red region of the spectrum. In addition to the minority carrier diffusion length change there is also a change

in the interface recombination velocity given by equation (84). This change can be related to the damage constant K_g by using equation (85)

$$S_g = S_{g_o}\left(\frac{L_{g_o}}{L_g}\right)^2 = S_{g_o}\left(1 + K_g L_{g_o}^2 \phi\right) \tag{86}$$

where S_{g_o} is the initial value of the interface recombination velocity and S_g is the value after irradiation with a fluence ϕ. Using the above model for radiation damage together with the device equations yields the theoretical curves of figures 17 and 18. These curves have the same character as the experimental data obtained from irradiating GaAlAs/GaAs heteroface solar cells with fluences of 10^{13}, 10^{14}, 10^{15} and 10^{16} 1 MeV electrons.

For shallow junction cells there will also be some damage in the base region, and we assume

$$\frac{1}{L_p^2} = \frac{1}{L_{p_o}^2} + K_p \phi$$

where K_p is a damage constant for the base region.

The radiation damage model was applied to GaAlAs/GaAs solar cells that had been exposed to 1 MeV electron fluences of 10^{13}, 10^{14}, 10^{15} and 10^{16} electrons/cm^2. Estimates of the initial values of the solar cell parameters were obtained from the computer minimization discussed earlier. These estimates in the initial values were not very accurate, as can be seen from figure 19 which is a numerical error analysis on the computed initial values of L_g and S_g. Despite the errors in the initial values an attempt was made to estimate a range of values for the damage coefficient K_g. For the cells that were tested the average damage constant was $K_g = 7.51(10^{-8})$ with a standard deviation of $\pm 6.93(10^{-8})$. This large standard deviation is due to the errors in the initial fitting of the solar cell parameters.

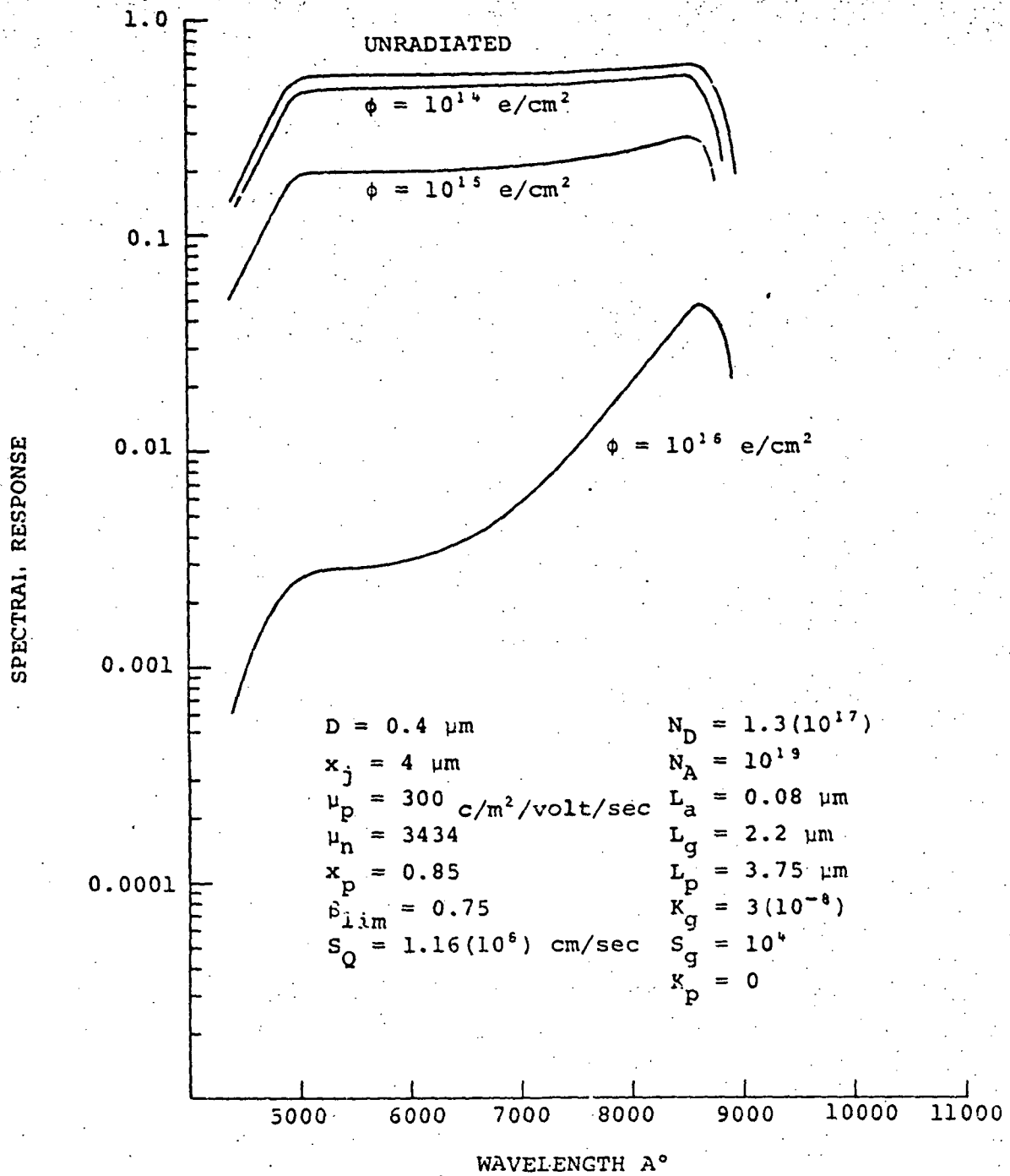

Figure 17. Theoretical spectral response curves from the radiation damage model and device equations.

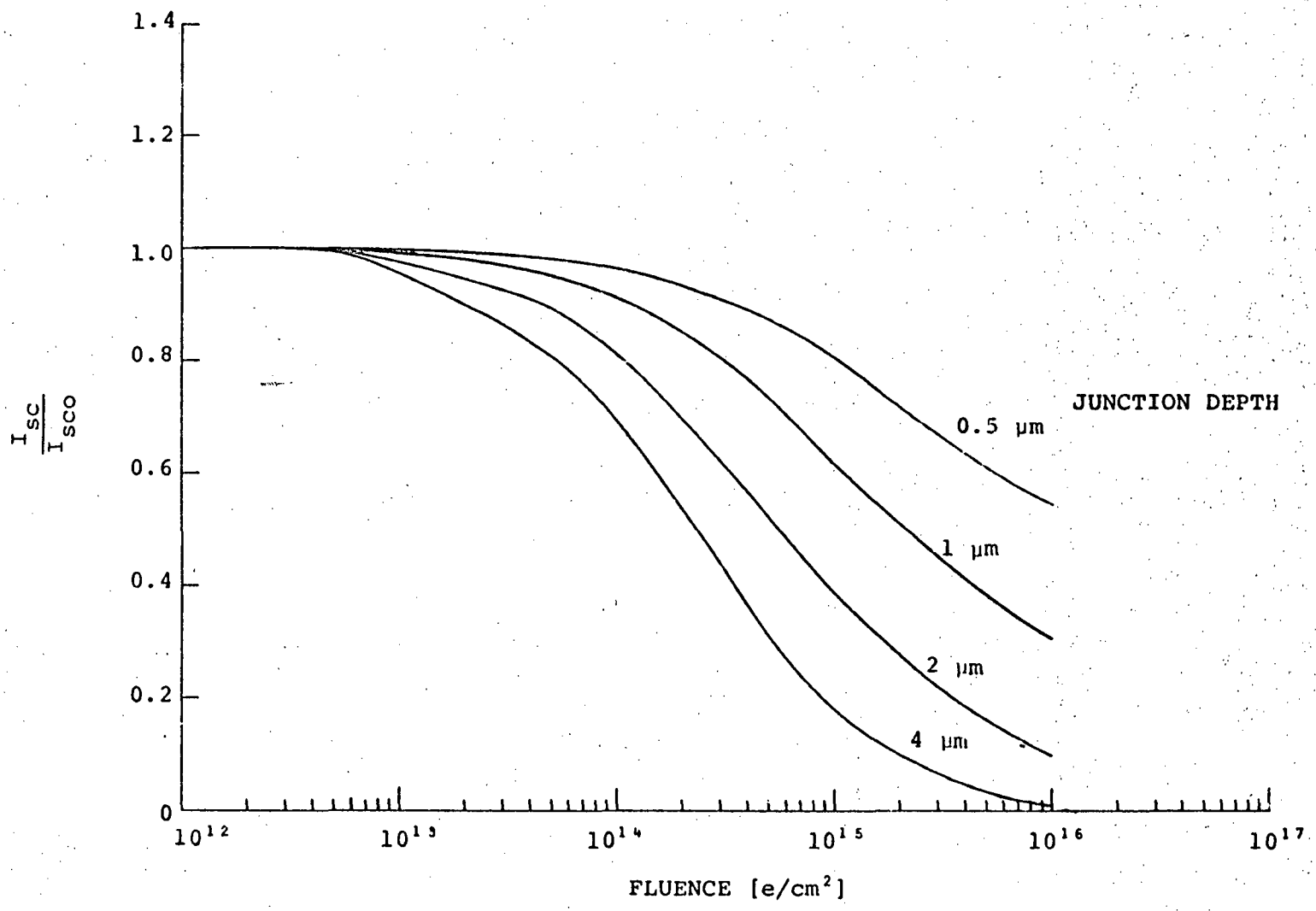

Figure 18. Theoretical curves for radiation damage for various junction depths.

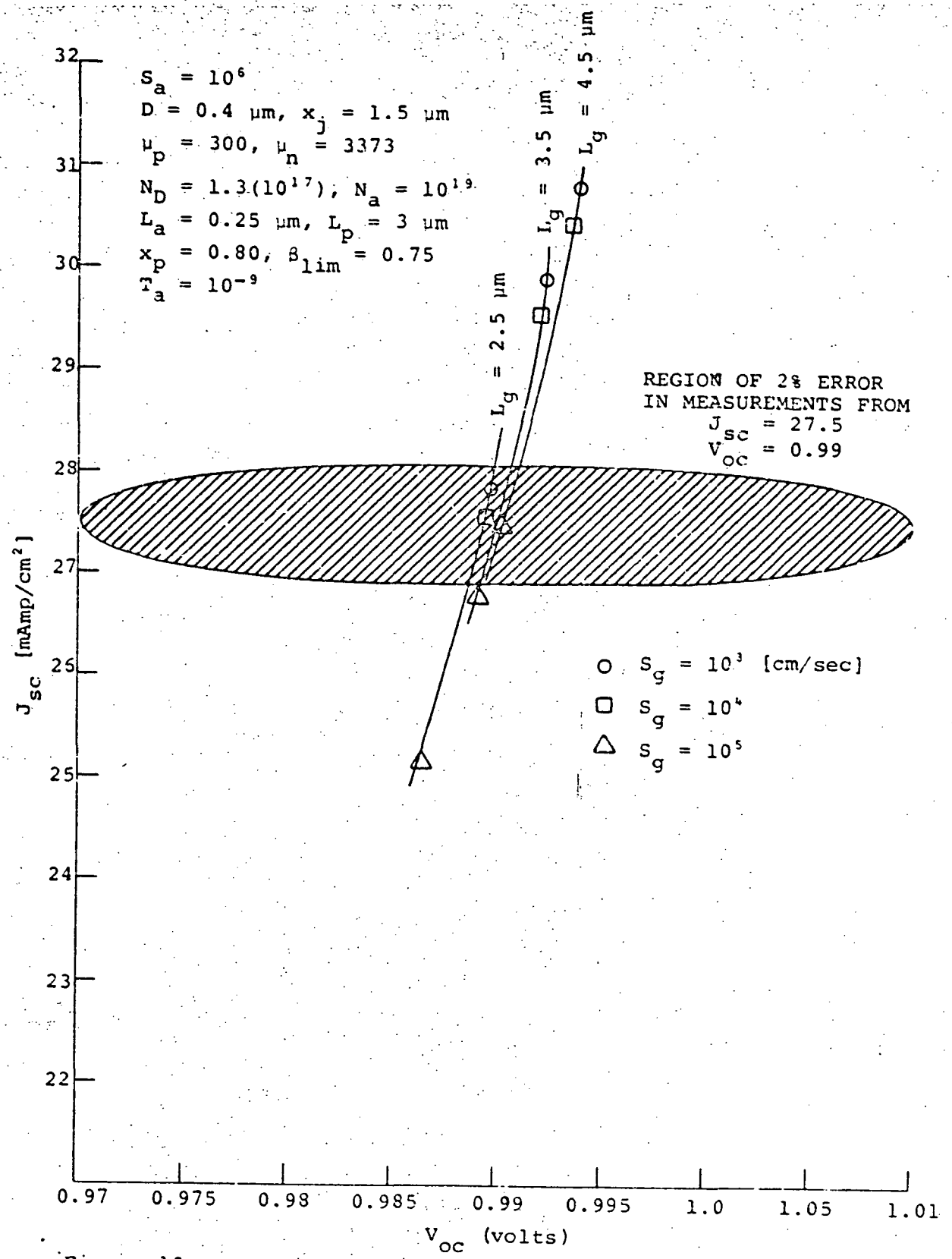

Figure 19. Error analysis on computed initial values of L_g and S_g.

The effect of the damage constant K_p on the spectral response curves is to lower the spectral response near the band edge. Since we were primarily trying to model deep junction cells which were not the kind one would use in an actual space experiment, the damage coefficient K_p was kept at zero.

Degradation of Electrical Properties

For GaAlAs/GaAs heteroface junction cells the quantum efficiency $Q(\lambda)$ given by equation (62) is the ratio of the photocurrent collected at wavelength λ to the number of photons incident upon the surface of the cell at wavelength λ. To a first approximation we will neglect the terms J_{D+x_j} and J_W occurring in equation (62). Also in equation (40) we will neglect the term J_D and assume $e^{-\alpha x_j}$ is very small. Then the collection efficiency before irradiation can be approximated by:

$$Q_o = Q_o\left(\alpha, L_{g_o}, x_j, S_{g_o}, \tau_{g_o}\right) = \frac{\alpha L_{g_o} e^{-\beta D}}{\alpha^2 L_{g_o}^2 - 1} \times \left[\frac{-\alpha L_{g_o} - \frac{\tau_{g_o} S_{go}}{L_{g_o}}}{\frac{S_{g_o} \tau_{g_o}}{L_{g_o}} \sinh\left(\frac{x_j}{L_{g_o}}\right) + \cosh\left(\frac{x_j}{L_{g_o}}\right)}\right] \tag{87}$$

(the zero subscript denoting initial value)
The collection efficiency after irradiation with fluence ϕ is then

$$Q_\phi = Q_\phi(\alpha, L_g, x_j, S_g, \tau_g) \tag{88}$$

where L_g and S_g after irradiation are given by equations (85) and (86). Further, since L_g is related to lifetime τ_g by $L_g^2 = D_g \tau_g$ we can write

$$\frac{1}{\tau_g} = \frac{1}{\tau_{g_o}} + D_g K_g \phi \tag{89}$$

we make the additional assumption that the change in short-circuit current rates is equal to the quantum efficiency ratio before and after irradiation. Then for a large absorption coefficient α we have the approximation

$$\frac{I_{sc}}{I_{sco}} = \frac{Q_\phi}{Q_o} \cong \frac{\frac{\tau_{g_o} S_{g_o}}{L_{g_o}} \sinh\left(\frac{x_j}{L_{g_o}}\right) + \cosh\left(\frac{x_j}{L_{g_o}}\right)}{\frac{\tau_g S_g}{L_g} \sinh\left(\frac{x_j}{L_g}\right) + \cosh\left(\frac{x_j}{L_g}\right)} . \tag{90}$$

Using equations (85), (86), (89), and (90) we assign the nominal values $K_g = 3.5(10^{-8})$, $\tau_{g_o} = 1.22(10^{-9})$, $S_{g_o} = 10^4$, $L_{g_o} = 3.25(10^{-4})$, $D_g = 86$. We can then vary the fluence ϕ and obtain figure 20.

This figure shows that the short-circuit current ratio is a function of fluence and junction depth. The curves in figure 20 are only approximate values, but they have the same general shape indicated by the experimental data.

The open-circuit voltage is related to the short-circuit current by relation

$$V_{oc} = \frac{AKT}{q} \ln\left(\frac{I_{sc}}{I_o} + 1\right) \tag{91}$$

where A is the perfection factor and I_o is the dark current. We may write

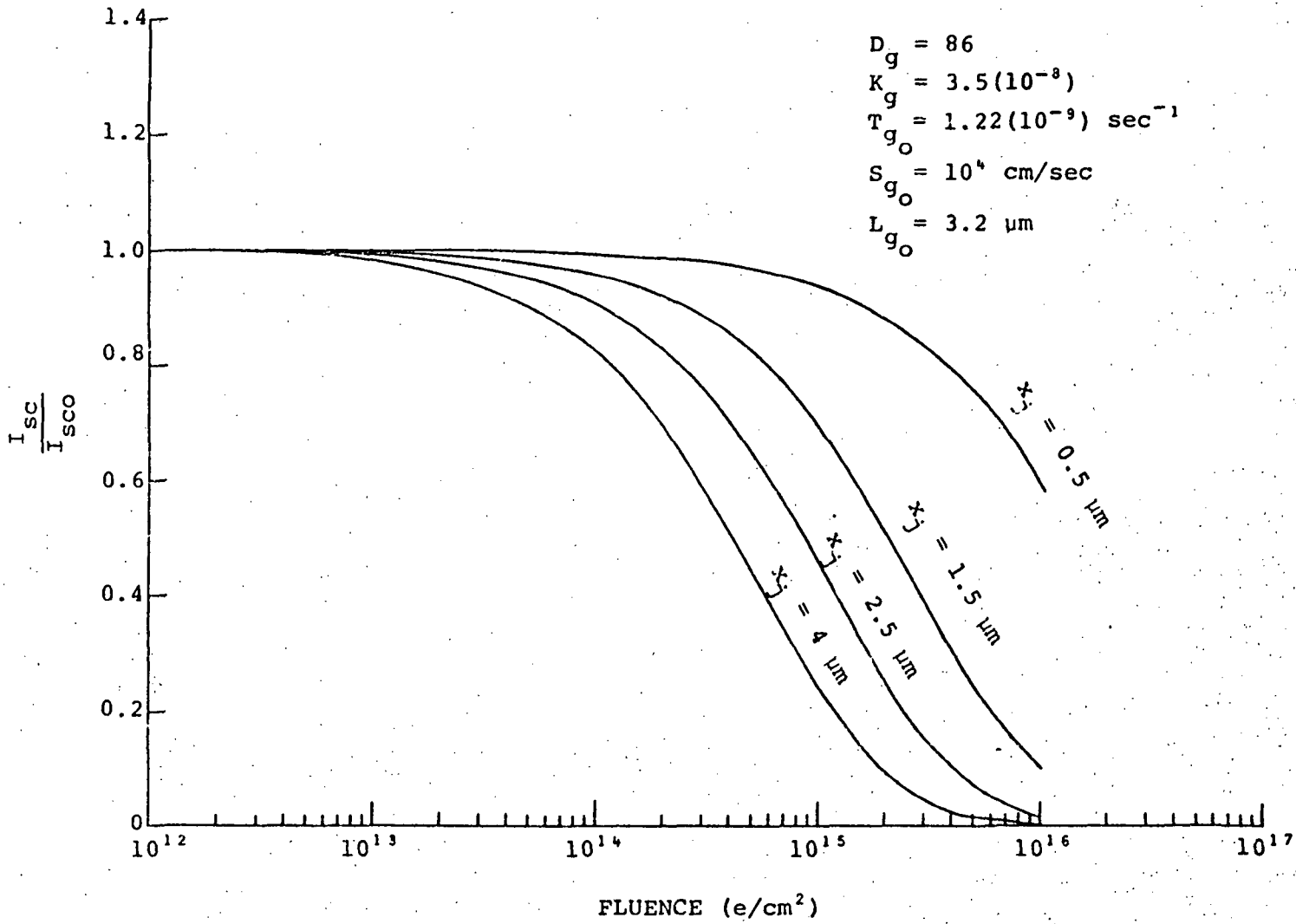

Figure 20. I_{sc}/I_{sco} model from equation (90) for various junction depths.

$$\frac{V_{oc}}{V_{oco}} = \frac{\ell n\left[\frac{I_{sc}}{I_o} + 1\right]}{\ell n\left[\frac{I_{sco}}{I_o} + 1\right]} = \frac{\ell n\left[\eta\ \frac{I_{sco}}{I_o} + 1\right]}{\ell n\left[\frac{I_{sco}}{I_o} + 1\right]} \qquad (92)$$

where $\eta = I_{sc}/I_{sco}$. Expanding the numerator in equation (92) as a Taylor series about $\eta = 1$ we obtain

$$\frac{V_{oc}}{V_{oco}} = 1 + K_1(\eta - 1) + K_2(\eta - 1)^2 + \ldots + K_n(\eta - 1)^n + \ldots \qquad (93)$$

where K_1, K_2,... are constants. We can also express equation (93) in the form

$$\frac{V_{oc}}{V_{oco}} = \alpha_0 + \alpha_1\left(\frac{I_{sc}}{I_{sco}}\right) + \alpha_2\left(\frac{I_{sc}}{I_{sco}}\right)^2 + \ldots \qquad (94)$$

where α_0, α_1, α_2,... are constants. This later equation also suggests a quadratic term in the statistical model for V_{oc}/V_{oco} as was developed earlier.

CONCLUSIONS

From the experimental and theoretical studies of GaAs solar cell behavior when exposed to 1 MeV electron fluences the following conclusions can be arrived at:

1. The models for I_{sc}/I_{sco} and V_{oc}/V_{oco}, developed for predictions of degradation due to effects of 1 MeV electron fluences, provide excellent fits to the data and will most likely provide good predictions within the experimental region ($1.5 \leq X_j \leq 4.0$) and ($10^{13} \leq \phi \leq 10^{16}$). As cell production procedures improve the experimental error will undoubtedly decrease and the derived prediction equations may be updated at that time, as the more improved data will reduce the prediction intervals and also the residual sum of squares of error will be reduced.

2. It must be emphasized that the limited number of cells used in this study were only test cells which were not radiation hardened. Hence, in the use of the prediction equations to estimate degradation effects in a space environment, the predictions will tend to overestimate the actual damage. Also effects of annealing are not incorporated into the prediction equations.

3. The theoretical studies and experimental results indicate that radiation hardened cells will be those cells with small junction depths (in the range from 0.2 to 0.5 μm)..

4. The theoretical studies and experimental studies on damage to the test cells indicate that 1 MeV electron fluences decrease the diffusion length L_g in the p-GaAs region while simultaneously increasing the recombination velocity S_g at the GaAlAs/GaAs interface.

5. In the design of a space experiment to actually test GaAs solar in a radiation environment the following items should be considered:

(a) Goals of experiment;

(b) Effects of shielding on electrical performance of solar cells in space;

(c) Effects of annealing on radiation damage and eventual electrical performance in space;

(d) Sample size to be tested in order to achieve significant statistical results;

(e) Accurate measurement of the parameters which affect results (i.e., measurements of equivalent 1 MeV electrons, temperature and annealing time); and

(f) Effects of annealing on electrical contacts and determination of probability of solar cell failure due to external causes as this probability will affect sample size on future experments in space.

REFERENCES

1. Woodall, J.M.; and Hovel, H.J.: Appl. Phys. Letters, vol. 30, no. 492, 1977.

2. Draper, N.R.; and Smith, M.: Applied Regression Analysis. John Wiley & Sons, Inc. (N.Y.), 1966.

3. Cochran, W.G.; and Cox, G.M.: Experimental Designs, 2nd Edition. John Wiley & Sons, Inc. (N.Y.), 1957.

4. Miller, R.G.: Simultaneous Statistical Inference. McGraw-Hill, Inc. (N.Y.), 1966.

5. Bancroft, T.A.: Topics in Intermediate Statistical Methods. The Iowa State Univ. Press (Ames, Iowa), 1968.

6. Netter, J.; and Wasserman, W.: Applied Linear Statistical Models. Irwin (Homewood, Ill.), 1974.

7. Hilberg, R.; Teaque, M.J.; and Vette, J.I.: Comparison of the Trapped Electron Models AE-4 and AE-5 with AE-2 and AE-3. NASA, Goddard Space Flight Center, NSSDC 74-13, Sept. 1974.

8. Walker, G.H.; Conway, E.J.: Annealing of GaAs Solar Cell Damage by Electron Irradiation. J. Electrochem. Soc., vol. 125, no. 4, Apr. 1978, pp. 676-677.

9. Hovel, H.J.: Semiconductor and Semimetals. Vol. II: Solar Cells. Academic Press (N.Y.), 1975.

10. Hovel, H.J. and Woodall, J.M.: Theoretical and Experimental Evaluations of $Ga_{1-X}Al_XAs$-GaAs Solar Cells. Rec. 10th IEEE Phot. Spec. Conf., Palo Alto, Calif., 1973.

11. The Solar Cell Array Design Handbook, vol. 1. Jet Prop. Lab., NASA, Oct. 1976.

12. Chaffin, R.J.: Microwave Semiconductor Devices: Fundamentals and Radiation Effects. John Wiley & Sons (N.Y.), 1973.

13. Hovel, H.J. and Woodall, J.M.: Optimization of Solar Cells for Air Mass Zero Operations and a Study of Solar Cells at High Temperatures. Final Report, NASA Contract NASI-12812, NASA-CR-145008, 1976.

14. Streetman, B.G.: Solid State Electronic Devices. Prentice Hall, Inc., 1972.

15. Corbett, J.W.: Electron Radiation Damage in Semiconductors and Metals. Academic Press (N.Y.), 1966.

16. Larin, F.: Radiation Effects in Semiconductor Devices. John Wiley & Sons, Inc. (N.Y.), 1968.

17. Cooley, W.C.; and Janda, R.J.; Handbook of Space Radiation Effects on Solar Cell Power Systems. NASA, SP-3003, 1963.

18. Walker, G.H.; Byvik, C.E.; Conway, E.J.; Heinbockel, J.H.; and Doviak, M.J.: Analytical and Experimental Study of 1 MeV Electron Irradiated GaAlAs/GaAs Heteroface Solar Cells. (Submitted to Electrochemical Society)

END

DATE

FILMED

JUL 20 1978